Structural systematics and conformational analyses of a 3 ´ 3 isomer grid of fluoro-*N*-(pyridyl)benzamides; physicochemical correlations, polymorphism and isomorphous relationships.

Pavle Mocilac, Katie Donnelly and John F. Gallagher*

Targeted Therapeutics and Theranostics (T^3) Programme, School of Chemical Sciences, Dublin City University, Dublin 9, Ireland

Correspondence E:mail *john.gallagher@dcu.ie*
Website: *http://doras.dcu.ie*

Electronic Supplementary Information

Table of Contents

1. Detailed description of synthetic procedures

All nine **Fxx** isomers were synthesised using standard nucleophilic acyl substitution reaction (Schotten-Baumann reaction) between the 4-/3-/2-aminopyridines and 4-/3-/2-fluorobenzoyl chlorides. In general, the procedure is as described for **Fxp** compounds in our previous publication (Donnelly *et al*., 2008). However, a different procedure was used for **Fxo**. The **Fxm** compounds were prepared by condensation reaction of 3-aminopyridine (3-AP) with 4-/3-/2-fluorobenzoyl chlorides in CH_2Cl_2 in the presence of one equivalent of triethylamine (Et_3N).

In a dry 100 ml round bottom flask, 3-aminopyridine (0.6219 g, 6.6 mmol) was dissolved with stirring in 50 ml of CH_2Cl_2 and Et_3N (1.394 ml, 10 mmol) was added. The flask with reaction mixture was placed on an ice bath and cooled. Under an inert atmosphere of N_2, the 4-/3-/2-fluorobenzoyl chlorides (mmol) were added and the reaction mixture stirred overnight. This mixture was washed three times with an aqueous $KHCO_3$ solution and the organic layer was dried with anhydrous $MgSO_4$. The solvent was removed by evaporation and the product was left to crystallise. A crystalline product was purified by column chromatography with silica as the stationary phase and using $CHCl_3$, ethyl acetate and acetone (2:2:1).

As the 2-aminopyridine (2-AP) has increased reactivity due to the *ortho* nitrogen and readily undergoes dibenzoylation reactions producing imides (Gallagher *et al*., 2009*a*,*b*) the syntheses of **Fxo** was based on the nucleophilic acyl substitution reaction between 2-AP and fluorobenzoyl chlorides, employing pyridine as a reaction medium without catalytic base and below a temperature of -10ºC.

The 2-aminopyridine (0.9412 g, 10 mmol) was added to a 100 ml two-neck round bottom flask placed on an ice bath (ice/water/NaCl/NH_4Cl) with stirring. Then, 30 ml of solvent (pyridine) was added to the flask. The flask was placed on ice bath and reaction mixture was allowed to cool to -10ºC. Finally, the 4-/3-/2-fluorobenzoyl chlorides (5 mmol) were added slowly into the solution mixture (depending on the reaction taking place). The reaction mixture was allowed to warm to room temperature and stirred overnight. Into the reaction mixture 100 ml of purified water was poured and *conc*. HCl was gradually added until a pH of 5-6 was obtained. A white precipitate was formed, and filtered on a Büchner's funnel. The precipitate was washed with copious amounts of water and allowed to dry. The pale yellow products were purified by column chromatography using standard procedures (**Fpo** and **Fmo**: silica//chloroform/ethyl acetate/*n*-hexane = 4:2:1; **Foo**: chloroform/ethyl acetate/*n*-hexane = 4:5:1).

Scheme 1. General reaction scheme of the **Fxx** reactions; The four **Fxx** conformations (below, right).

$$FC_6H_4COCl + H_2NC_5H_4N \rightarrow FC_6H_4CONHC_5H_4N$$

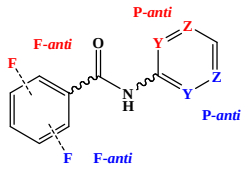

Table 1. Resulting quantities, yields and melting points of **Fxx** compounds.

Fxx	m/g	yield/%	m.p./ºC
Fpp	1.160	81.3	186.1-187.8
Fmp	1.133	79.4	185.0-186.6
Fop	3.711	86.7	134.7-135.6
Fpm	1.097	76.9	148.8-149.1
Fmm	1.046	73.3	149.7-152.2
Fom	1.926	67.5	89.2-89.6
Fpo	0.771	54.0	117.2-123.1
Fmo	1.275	59.0	76.7-77.4
Foo	1.567	36.2	84.0-86.1

2. ^{1}H NMR data and spectra

2.1 Fpp

^{1}H NMR ($CDCl_3$) δ 7.12 (2H, tt, ^{3}J = 8.5, ^{4}J = 2.5), 7.53 (2H, dd, ^{3}J = 5.0, ^{4}J = 1.5), 7.83 (2H, ddt, 2H, ddt, ^{3}J = 8.8, ^{4}J = 5.2, ^{5}J = 2.5), 8.01 (1H, br s), 8.48 (2H, dd, ^{3}J = 4.8, ^{4}J = 1.5); **^{1}H NMR (DMSO-d_6)** δ 7.40 (2H, t, ^{3}J = 8.8), 7.78 (2H, dd, ^{3}J = 5, ^{4}J = 1.5), 8.05 (2H, dd, ^{3}J = 8.8, ^{4}J = 5.5), 8.48 (2H, dd, ^{3}J = 6), 10.61 (1H, br s); **^{13}C NMR (DMSO-d_6)** δ 113.98, 115.36/115.58, 130.62/130.71, 130.63/130.66, 145.82, 150.29, 163.09/165.57, 165.32; **^{19}F NMR (DMSO-d_6)** δ -107.84 (1H, m);

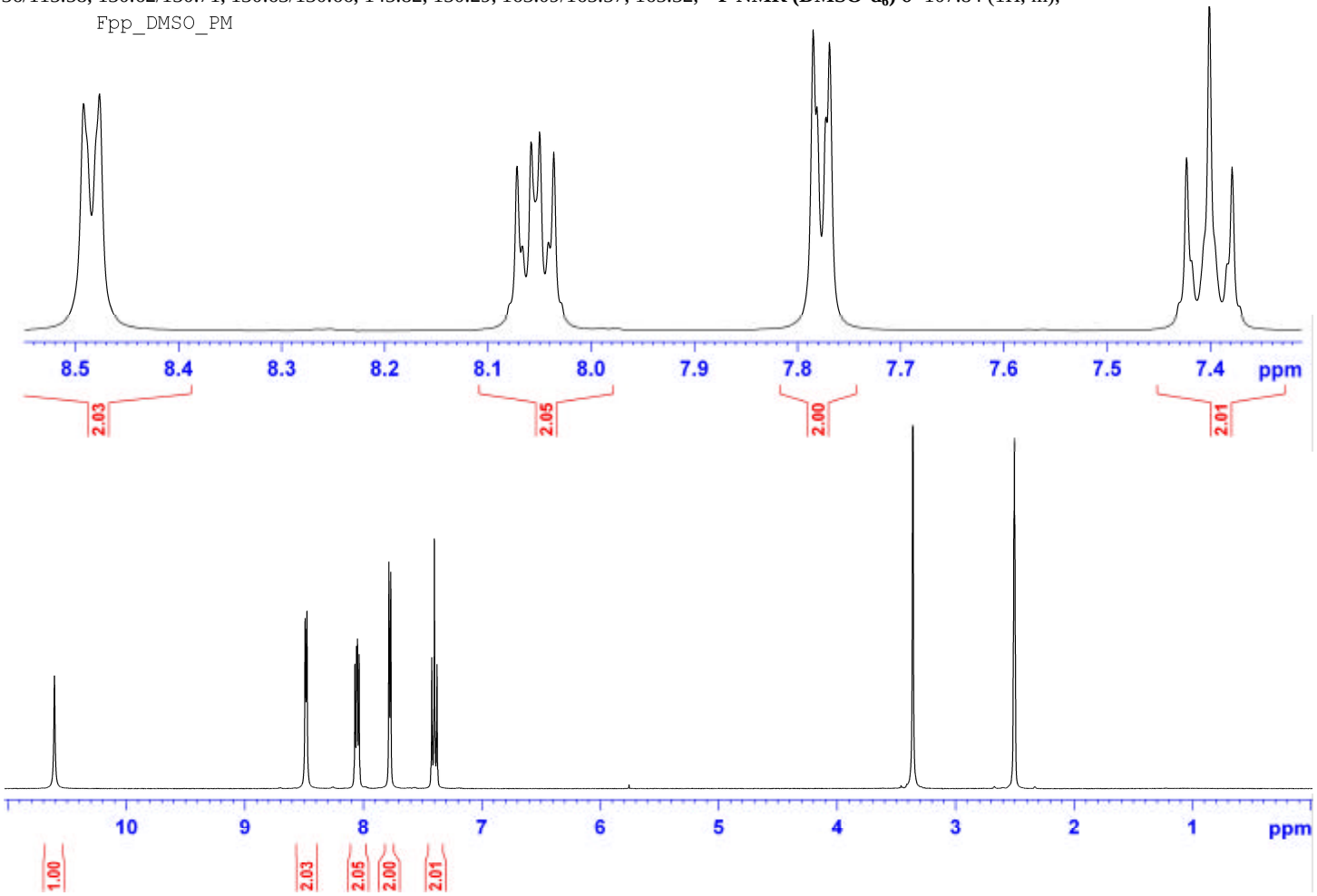

2.2 Fmp

^{1}H NMR ($CDCl_3$) δ 7.23 (1H, tdd, ^{3}J = 8.3, ^{4}J = 2.5, ^{5}J = 0.8), 7.43 (1H, td, ^{3}J = 8.3, ^{4}J = 5.4), 7.53 (1H, ddd, ^{3}J = 9.2, ^{4}J = 2.7, ^{5}J = 1.7), 7.54 (2H, dd, ^{3}J = 4.8, ^{4}J = 1.5), 7.58 (1H, ddd; ^{3}J = 7.8, ^{4}J = 1.7, ^{5}J = 1.0), 8.01 (1H, br s), 8.49 (2H, dd, ^{3}J = 4.8, ^{4}J = 1.5); **^{1}H NMR (DMSO-d_6)** δ 7.49 (1H, tdd, ^{3}J = 8.3, ^{4}J = 2.5, ^{5}J = 0.8), 7.62 (1H, td, ^{3}J = 8.0, ^{4}J = 5.8), 7.78 (2H, dd, ^{3}J = 4.6, ^{4}J = 1.6), 7.79 (1H, ddd, ^{3}J = 9.8, ^{4}J = 2.6, ^{5}J = 1.6), 7.82 (1H, dt, ^{3}J = 7.8, ^{4}J = 1.2), 8.49 (2H, dd, ^{3}J = 4.5, ^{4}J = 1.5), 10.66 (1H, br s); **^{13}C NMR (DMSO-d_6)** δ 114.04, 114.55/114.78, 118.90/119.12, 124.06/124.09, 130.68/130/76, 136.41/136.46, 145.64, 150.32, 160.64/163.08, 165.08; **^{19}F NMR (DMSO-d_6)** δ -112.42 (1F, m);

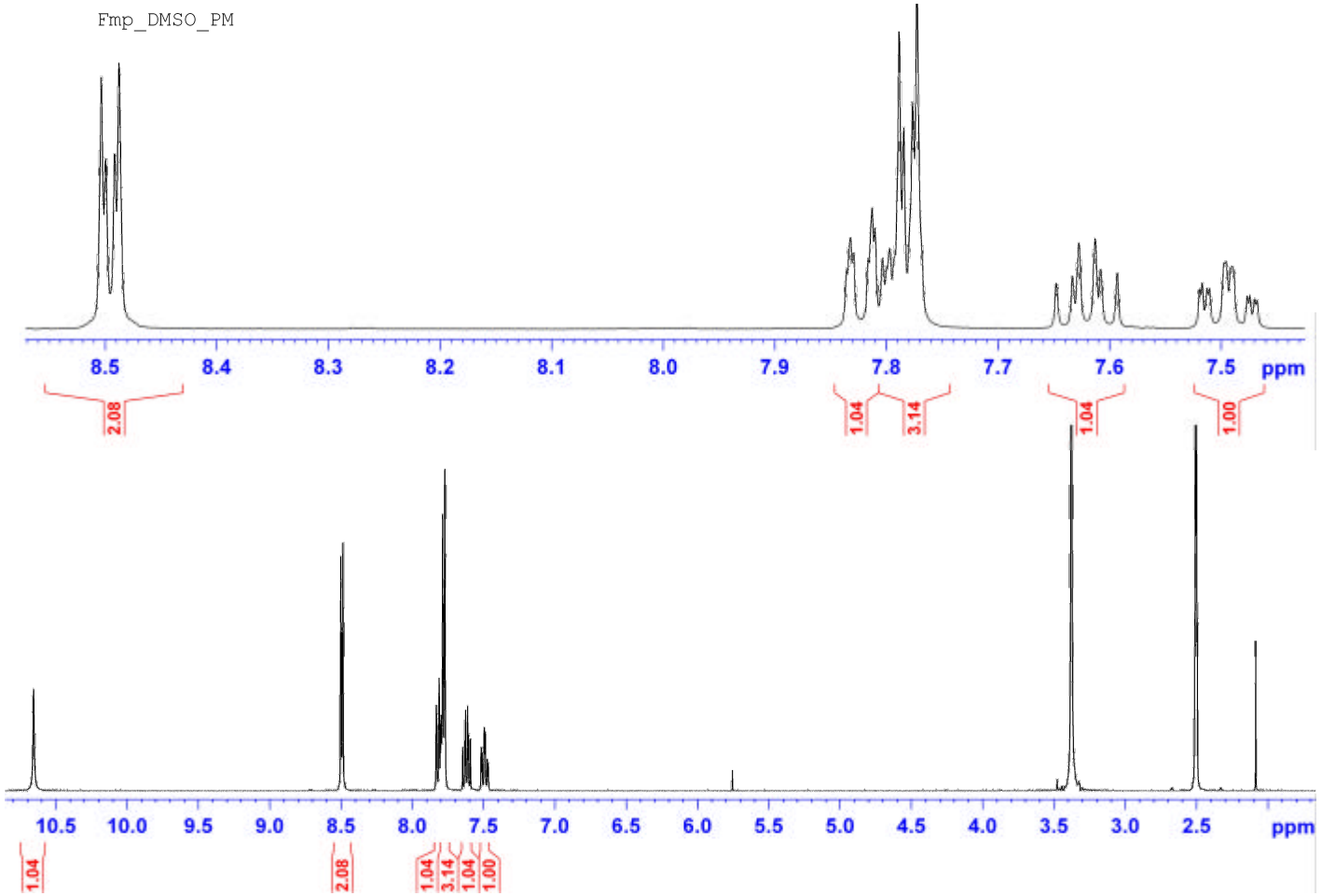

2.3 Fop

^{1}H NMR ($CDCl_3$) δ 7.22 (1H, ddd, ^{3}J = 12, ^{4}J = 8.4, ^{5}J = 0.8), 7.35 (1H, td, ^{3}J = 7.7, ^{4}J = 1), 7.58 (1H, m), 7.64 (2H, dd, ^{3}J = 4.9, ^{4}J = 1.6), 8.16 (1H, td, ^{3}J = 8.0, ^{4}J = 1.8), 8.56 (2H, dd, ^{3}J = 5.0, ^{4}J = 1.6), 8.68 (1H, br d, $^{1h}J_{N–H...F}$ = 15.5); **^{1}H NMR (DMSO-d_6)** δ 7.36 (1H, td, ^{3}J = 7.6, ^{4}J = 1.0) 7.38 (1H, ddd, ^{3}J = 12, ^{4}J = 8.5, ^{5}J = 0.9), 7.62 (1H, m), 7.70 (1H, td, ^{3}J = 8.0, ^{4}J = 1.8), 7.7 (2H, dd, 1H, td, ^{3}J = 5.0, ^{4}J = 1.6), 8.49 (2H, dd, ^{3}J = 5.0, ^{4}J = 1.5), 10.82 (1H, br s); **^{13}C NMR (DMSO-d_6)** δ 113.60, 116.13/116.34, 124.17/124.31, 124.63/124.66, 129.90/129.93, 133.01/133.09, 145.38, 150.45, 157.62/160.10, 163.75; **^{19}F NMR (DMSO-d_6)** δ -114.52 (1F, m).

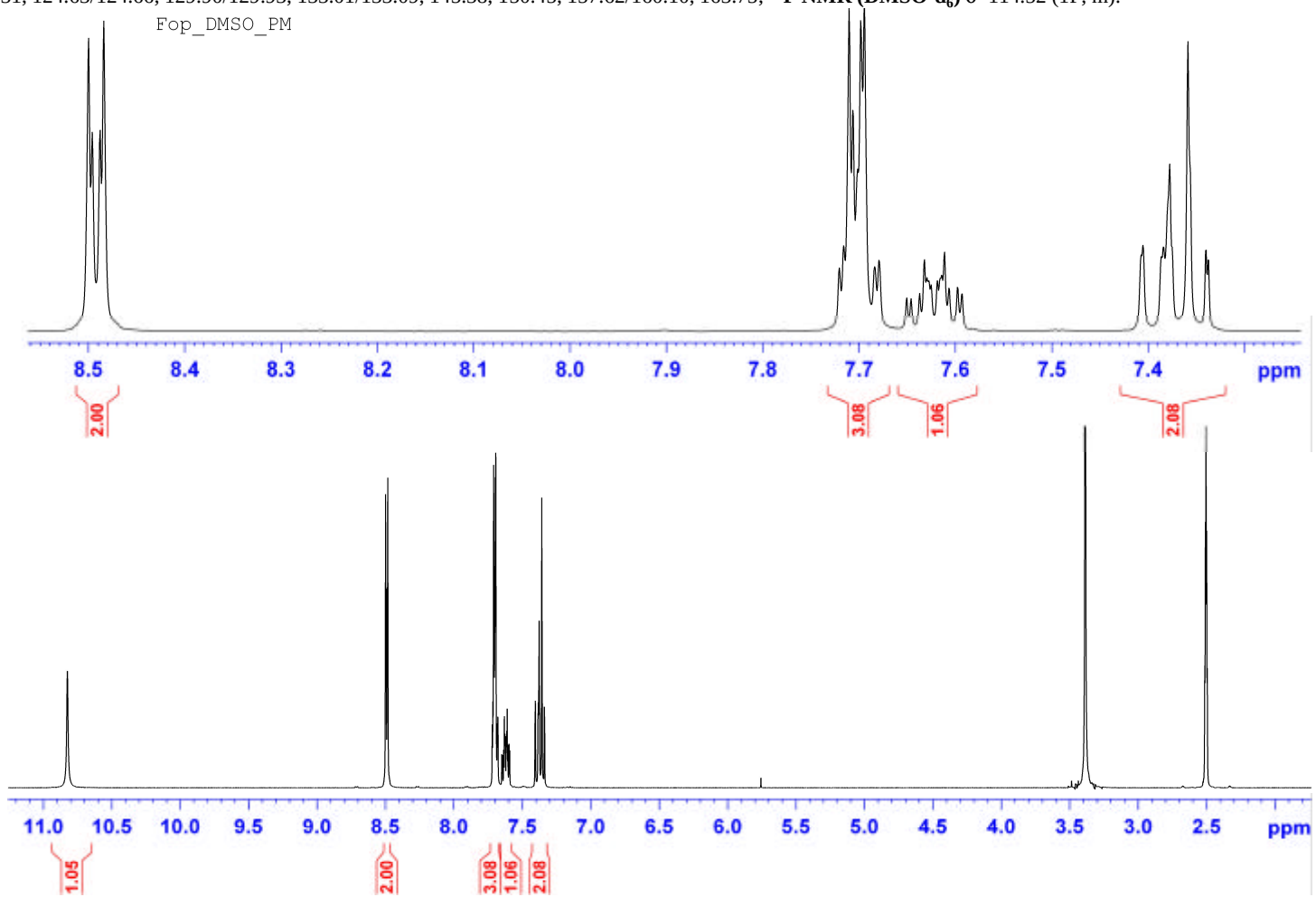

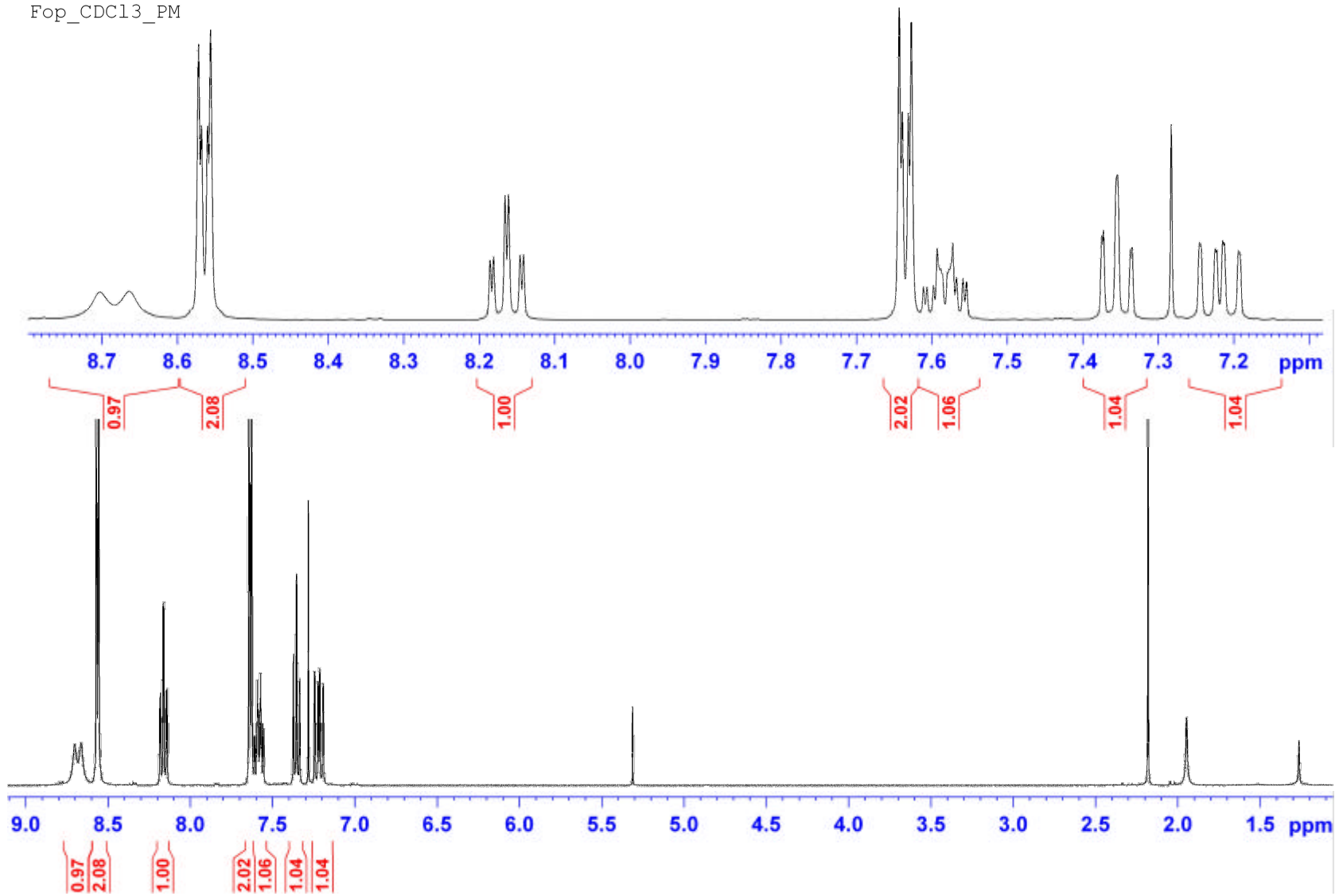
Fop_CDCl3_PM
8.7
8.6
8.5
8.4
8.3
8.2
8.1
8.0
7.9
7.8
7.7
7.6
7.5
7.4
7.3
7.2
ppm
0.97
2.08
1.00
2.02
1.06
1.04
1.04
9.0
8.5
8.0
7.5
7.0
6.5
6.0
5.5
5.0
4.5
4.0
3.5
3.0
2.5
2.0
1.5
ppm
0.97
2.08
1.00
2.02
1.06
1.04
1.04

2.4. Fpm

^{1}H NMR ($CDCl_3$) δ 7.07 (2H, tt, ^{3}J = 8.5, ^{4}J = 2.5), 7.25 (1H, dd, ^{3}J = 8.5, ^{4}J = 4.9), 7.86 (2H, ddt, ^{3}J = 8.7, ^{4}J = 5.2, ^{5}J = 2.5), 8.25 (1H, ddd, ^{3}J = 8.5, ^{4}J = 2.5, ^{5}J = 1.4), 8.25 (1H, dd, ^{3}J = 4.8, ^{4}J = 1.2), 8.56 (1H, br s), 8.64 (1H, s); **^{1}H NMR (DMSO-d_6)** δ 7.40 (1H, ddd, ^{3}J = 8.4, ^{4}J = 4.7, ^{5}J = 0.5), 7.40 (2H, tt, ^{3}J = 8.9, ^{4}J = 2.5), 8.06 (2H, ddt, ^{3}J = 8.8, ^{4}J = 5.4, ^{5}J = 2.5), 8.18 (1H, ddd, ^{3}J = 8.4, ^{4}J = 2.5, ^{5}J =1.4), 8.32 (1H, dd, ^{3}J = 4.6, ^{4}J = 1.4), 8.92 (1H, d, ^{3}J = 2.4), 10.47 (1H, br s); **^{13}C NMR (DMSO-d_6)** δ 115.31/115.53, 123.51, 127.35, 130.44/130.52, 130.73/130.76, 135.69, 141.97, 144.61, 162.97/165.45, 164.80; **^{19}F NMR (DMSO-d_6)** δ -108.27 (1F, m).

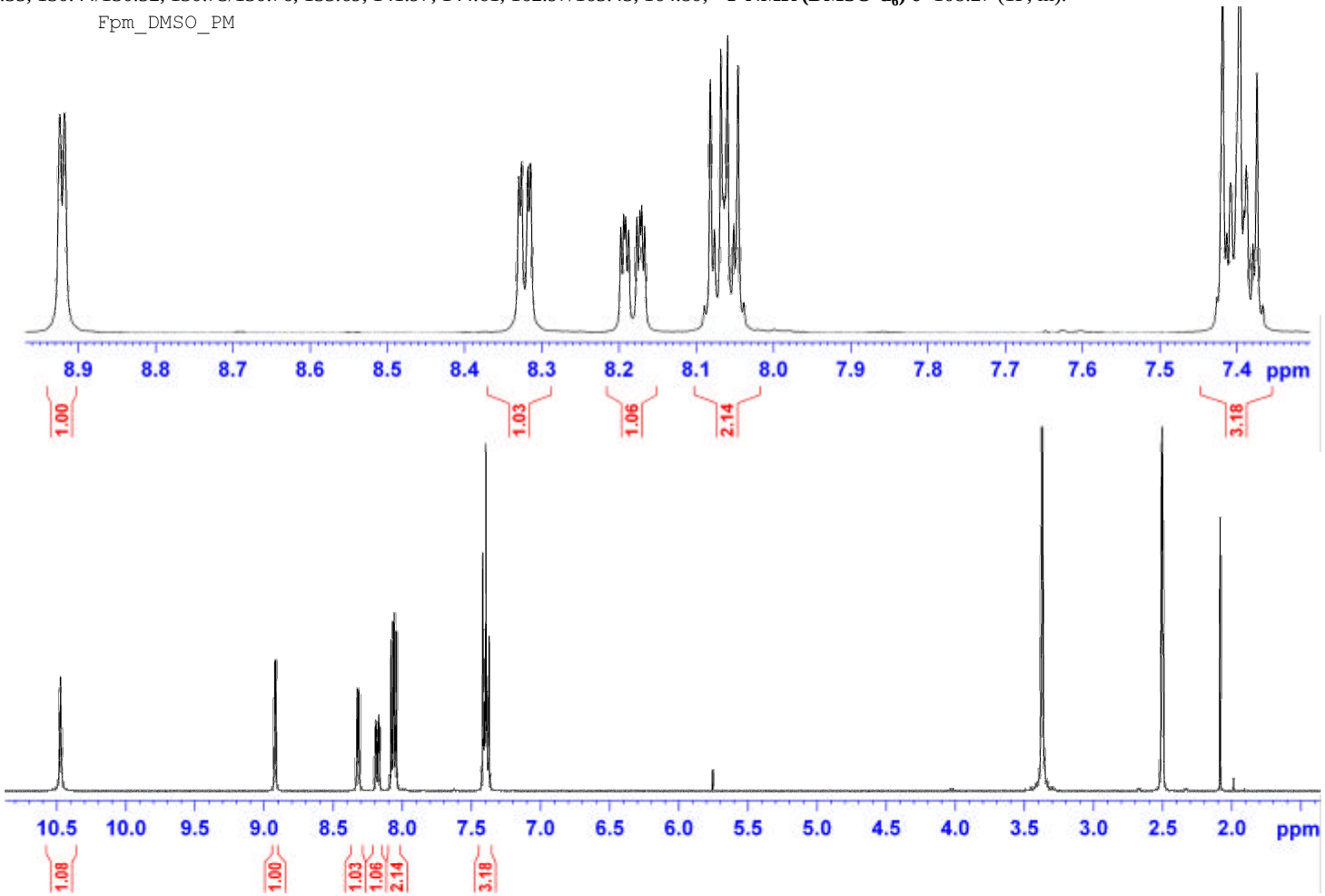

2.5. Fmm

^{1}H NMR ($CDCl_3$) δ 7.19 (1H, tdd, ^{3}J = 8.3, ^{4}J = 2.6, ^{5}J = 0.8), 7.28 (1H, dd, ^{3}J = 8.4, ^{4}J = 5.0), 7.39 (1H, td, ^{3}J = 8.2, ^{4}J = 5.5), 7.57 (1H, ddd, ^{3}J = 9.2, ^{4}J = 2.7, ^{5}J = 1.7), 7.62 (1H, ddd, ^{3}J = 7.7, ^{4}J = 1.6, ^{5}J = 1.0), 8.28 (1H, ddd, ^{3}J = 8.5, ^{4}J = 2.5, ^{5}J = 1.4) 8.28 (1H, dd, ^{3}J = 4.8, ^{4}J = 1.2), 8.45 (1H, br s), 8.68 (1H, d, ^{3}J = 2.3); **^{1}H NMR ($DMSO-d_6$)** δ 7.41 (1H, ddd, ^{3}J = 8.4, ^{4}J = 4.7, ^{5}J = 0.5), 7.48 (1H, tdd, ^{3}J = 8.6, ^{4}J = 2.6, ^{5}J = 1.0), 7.62 (1H, td, ^{3}J = 8.3, ^{4}J = 5.8), 7.80 (1H, ddd, ^{3}J = 9.8, ^{4}J = 2.7, ^{5}J = 1.6), 7.84 (1H, dt, ^{3}J = 7.8, ^{4}J = 1.2), 8.19 (1H, ddd, ^{3}J = 8.4, ^{4}J = 2.6, ^{5}J = 1.5), 8.33 (1H, dd, ^{3}J = 4.7, ^{4}J = 1.5), 8.93 (1H, d, ^{3}J = 2.5), 10.53 (1H, br s); **^{13}C NMR ($DMSO-d_6$)** δ 114.42/114.65, 118.67/118.88, 123.55, 123.92/123.94, 127.41, 130.64/130.72, 135.52, 136.55/136.62, 142.00, 144.78, 160.68/163.11, 164.53; **^{19}F NMR ($DMSO-d_6$)** δ -112.50 (1F, m).

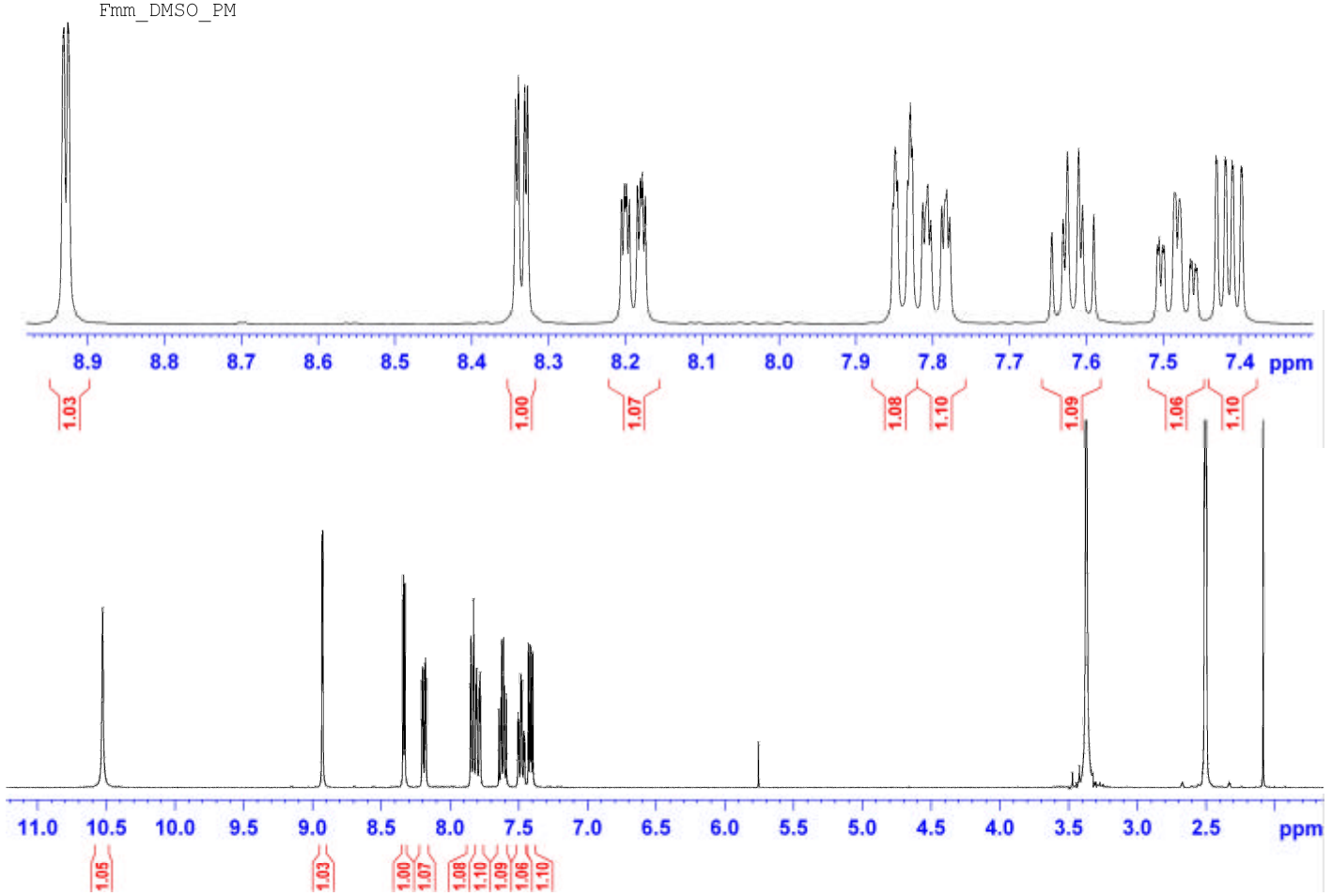

2.6. Fom

^{1}H NMR ($CDCl_3$) δ 7.13 (1H, ddd, ^{3}J = 12.3, ^{4}J = 8.4, ^{5}J = 0.8), 7.25 (1H, td, ^{3}J = 7.7, ^{4}J = 1), 7.26 (1H, dd, ^{3}J = 8.5, ^{4}J = 4.9), 7.48 (1H, m), 8.08 (1H, td, ^{3}J = 7.9, ^{4}J = 1.8), 8.23 (1H, ddd, ^{3}J = 8.3, ^{4}J = 2.7, ^{5}J = 1.5), 8.33 (1H, d, ^{3}J = 4.2), 8.53 (1H, br d, $^{1h}J_{N-H...F}$ = 15.3), 8.64 (1H, d, ^{3}J = 1.6); **^{1}H NMR (DMSO-d_6)** δ 7.36 (1H, td, ^{3}J = 7.6, ^{4}J = 1.0) 7.38 (1H, ddd, ^{3}J = 12, ^{4}J = 8.5, ^{5}J = 0.9), 7.41 (1H, dd, ^{3}J = 8.7, ^{4}J = 4.7), 7.61 (1H, m), 7.71 (1H, td, ^{3}J = 7.5, ^{4}J = 1.7), 8.17 (1H, ddd, ^{3}J = 8.2, ^{4}J = 2.5, ^{5}J = 1.4), 8.33 (1H, dd, ^{3}J = 4.5, ^{4}J = 1.3), 8.88 (1H, d, ^{3}J = 2.2), 10.68 (1H, br s); **^{13}C NMR (DMSO-d_6)** δ 116.11/116.33, 123.66, 124.29/124.44, 124.59/124.63, 126.68, 129.91/129.94, 132.80/132.89, 135.50, 141.23, 144.77, 157.65/160.13, 163.19; **^{19}F NMR (DMSO-d_6)** δ -114.49 (1F, m).

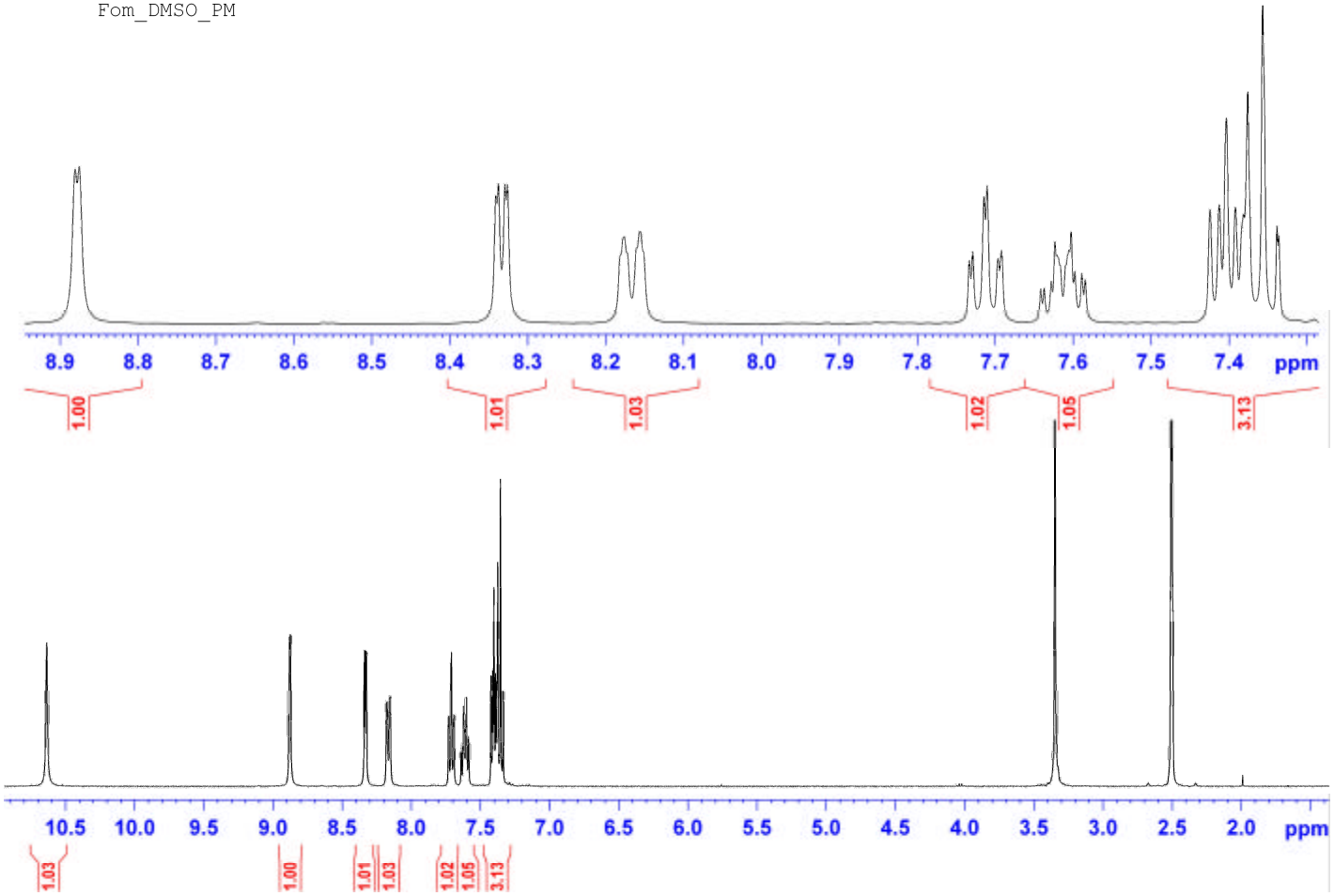

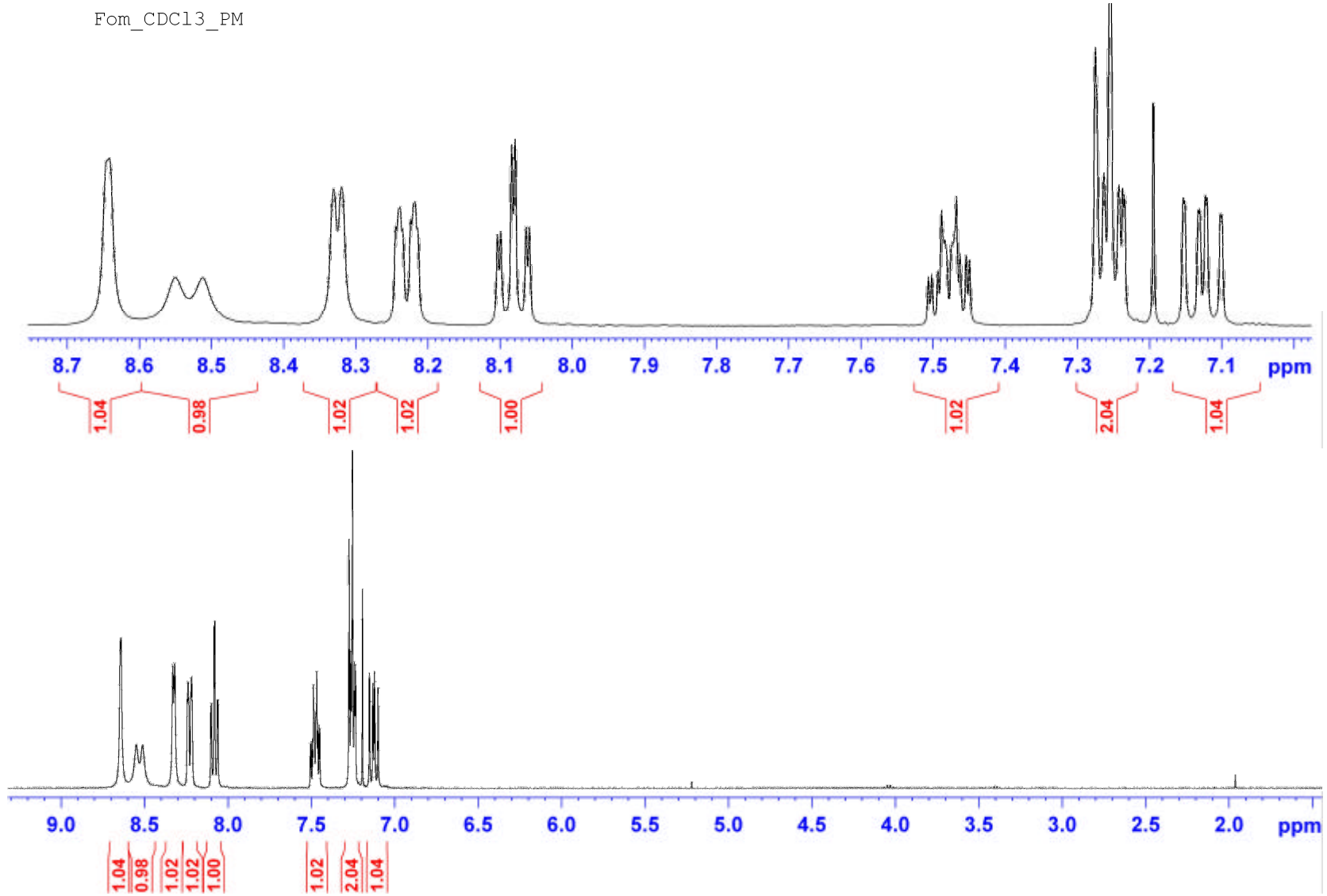
Fom_CDCl3_PM
8.7 8.6 8.5 8.4 8.3 8.2 8.1 8.0 7.9 7.8 7.7 7.6 7.5 7.4 7.3 7.2 7.1 ppm
1.04 0.98 1.02 1.02 1.00 1.02 2.04 1.04
9.0 8.5 8.0 7.5 7.0 6.5 6.0 5.5 5.0 4.5 4.0 3.5 3.0 2.5 2.0 ppm
1.04 0.98 1.02 1.02 1.00 1.02 2.04 1.04

2.7. Fpo

^{1}H NMR ($CDCl_3$) δ 7.02 (1H, ddd, ^{3}J = 7.5, ^{4}J = 5.3, ^{5}J = 0.7), 7.11 (2H, t, ^{3}J = 8.5), 7.33 (1H, td, ^{3}J = 7.8, ^{4}J = 1.8), 7.91 (2H, ddt, ^{3}J = 8.7, ^{4}J = 5.2, ^{5}J = 2.5), 8.17 (1H, d, ^{3}J = 4.7), 8.34 (1H, d, ^{3}J = 8.4), 9.04 (1H, br s); **^{1}H NMR (DMSO-d_6)** δ 7.17 (1H, ddd, ^{3}J = 7.4, ^{4}J = 4.9, ^{5}J = 0.8), 7.35 (2H, t, ^{3}J = 8.9), 7.85 (1H, td, ^{3}J = 7.8, ^{4}J = 1.9), 8.11 (2H, ddt, ^{3}J = 8.8, ^{4}J = 5.5, ^{5}J = 2.5), 8.18 (1H, d, ^{3}J = 8.3), 8.39 (1H, ddd, ^{3}J = 4.6, ^{4}J = 1.7, ^{5}J = 0.8), 10.87 (1H, br s); **^{13}C NMR (DMSO-d_6)** δ 114.70, 115.17/115.39, 119.84, 130.49/130.52, 130.73/130.82, 138.12, 147.91, 152.10, 163.01/165.50, 164.90; **^{19}F NMR (DMSO-d_6)** δ -108.23 (1F, m).

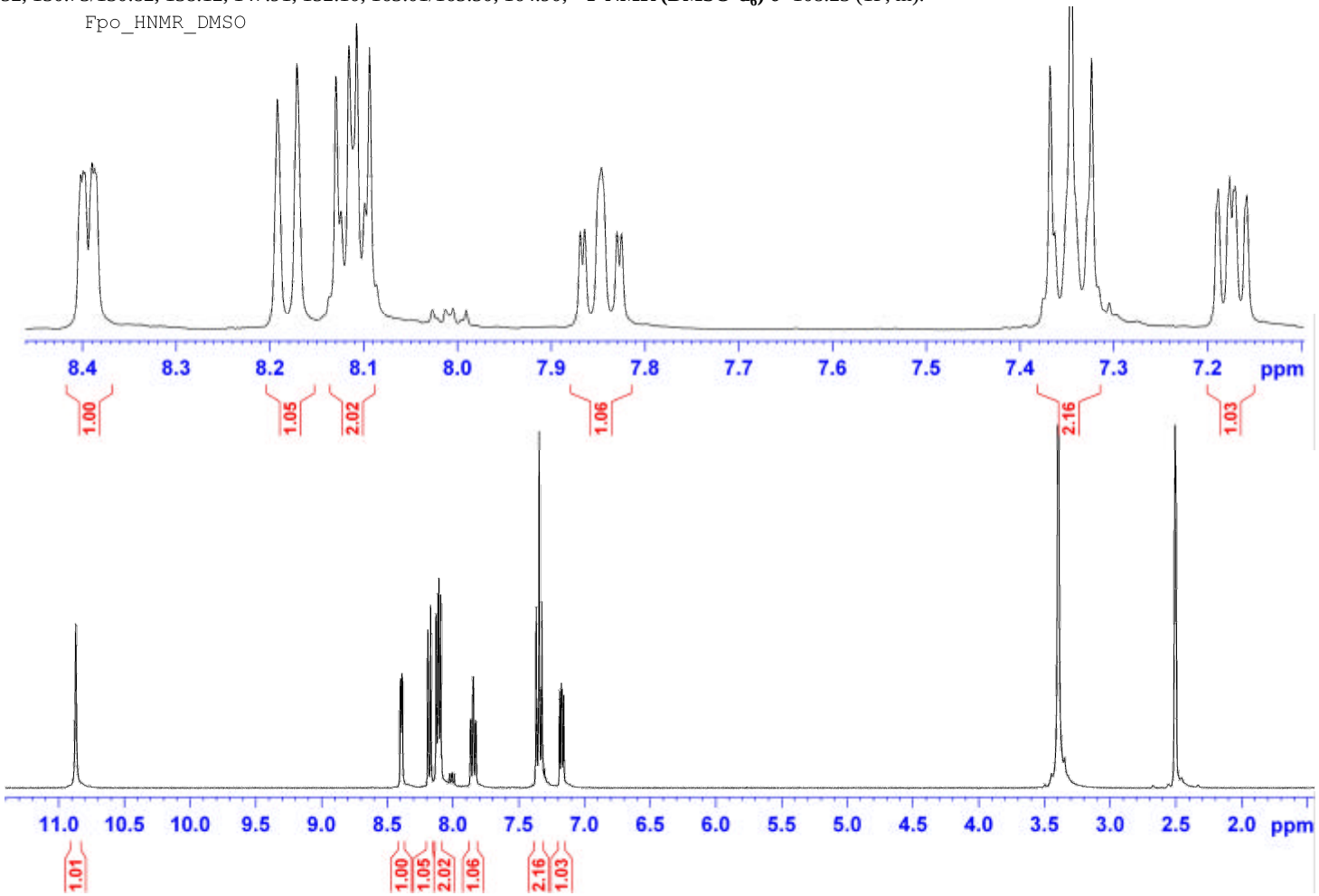

2.8 Fmo

^{1}H NMR ($CDCl_3$) δ 7.01 (1H, ddd, ^{3}J = 7.5, ^{4}J = 4.9, ^{5}J = 0.8), 7.19 (1H, tdd, ^{3}J = 8.3, ^{4}J = 2.6, ^{5}J = 0.8), 7.39 (1H, td, ^{3}J = 8.2, ^{4}J = 5.4), 7.58 (1H, ddd, ^{3}J = 9.2, ^{4}J = 2.6, ^{5}J = 1.7), 7.61 (1H, ddd, ^{3}J = 7.7, ^{4}J = 1.6, ^{5}J = 1.0), 7.70 (1H, td, ^{3}J = 7.8, ^{4}J = 1.9), 8.17 (1H, d, ^{3}J = 4.8), 8.30 (1H, d, ^{3}J = 8.4), 8.75 (1H, br s); **^{1}H NMR ($DMSO-d_6$)** δ 7.19 (1H, ddd, ^{3}J = 7.5, ^{4}J = 4.8, ^{5}J = 1.0), 7.45 (1H, tdd, ^{3}J = 8.5, ^{4}J = 2.6, ^{5}J = 0.9), 7.57 (1H, td, ^{3}J = 8.2, ^{4}J = 5.8), 7.85 (1H, ddd, ^{3}J = 9.8, ^{4}J = 2.7, ^{5}J = 1.6), 7.86 (1H, td, ^{3}J = 7.8, ^{4}J = 1.9), 7.89 (1H, dt, ^{3}J = 7.8, ^{4}J = 1.2), 8.18 (1H, d, ^{3}J = 8.4), 8.4 (1H, ddd, ^{3}J = 4.9, ^{4}J = 2.0, ^{5}J = 0.7), 10.90 (1H, br s); **^{13}C NMR ($DMSO-d_6$)** δ 114.74/114.97, 114.84, 118.74/118.95, 120.04, 124.22/124.24, 130.49/130.56, 136.37/136.44, 138.20, 148.00, 151.99, 160.67/163.09, 164.69; **^{19}F NMR ($DMSO-d_6$)** δ -112.57 (1F, m).

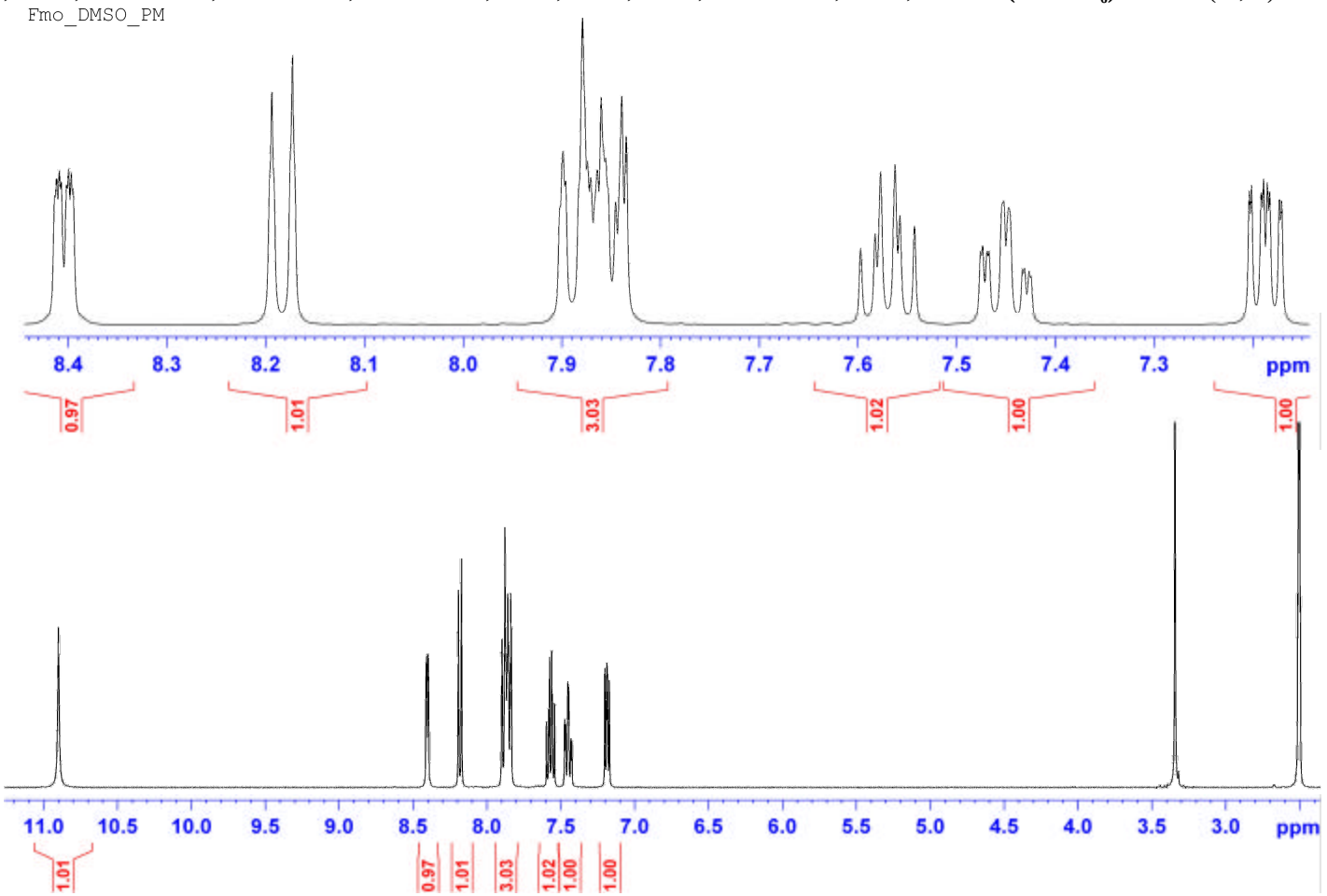

2.9 Foo

^{1}H NMR ($CDCl_3$) δ 7.01 (1H, ddd, ^{3}J = 7.5, ^{4}J = 4.9, ^{5}J = 0.9), 7.13 (1H, ddd, ^{3}J = 12, ^{4}J = 8.3, ^{5}J = 1.0), 7.25 (1H, td, ^{3}J = 7.6, ^{4}J = 1.0), 7.47 (1H, m), 7.69 (1H, td, ^{3}J = 8.0, ^{4}J = 1.9), 8.08 (1H, td, ^{3}J = 7.9, ^{4}J = 1.9), 8.25 (1H, d, ^{3}J = 4.3), 8.32 (1H, d, ^{3}J = 8.5), 9.03 (1H, br d, $^{1h}J_{N–H...F}$ = 13.0); **^{1}H NMR ($DMSO-d_6$)** δ 7.18 (1H, ddd, ^{3}J = 7.5, ^{4}J = 4.9, ^{5}J = 0.9), 7.32 (1H, td, ^{3}J = 7.6, ^{4}J = 1.0), 7.33 (1H, ddd, ^{3}J = 12, ^{4}J = 8.3, ^{5}J = 1.0), 7.59 (1H, m), 7.71 (1H, td, ^{3}J = 7.5, ^{4}J = 1.7), 7.86 (1H, td, ^{3}J = 8.0, ^{4}J = 1.9), 8.19 (1H, d, ^{3}J = 8.4), 8.37 (1H, ddd, ^{3}J = 4.9, ^{4}J = 1.6, ^{5}J = 0.8), 10.78 (1H, br s); **^{13}C NMR ($DMSO-d_6$)** δ 114.09, 115.99/116.21, 120.01, 124.01/124.16, 124.44/124.47, 130.10/130.13, 132.84/132.92, 138.29, 148.10, 151.64, 157.90/160.37, 163.31; **^{19}F NMR ($DMSO-d_6$)** δ -114.03 (1F, m).

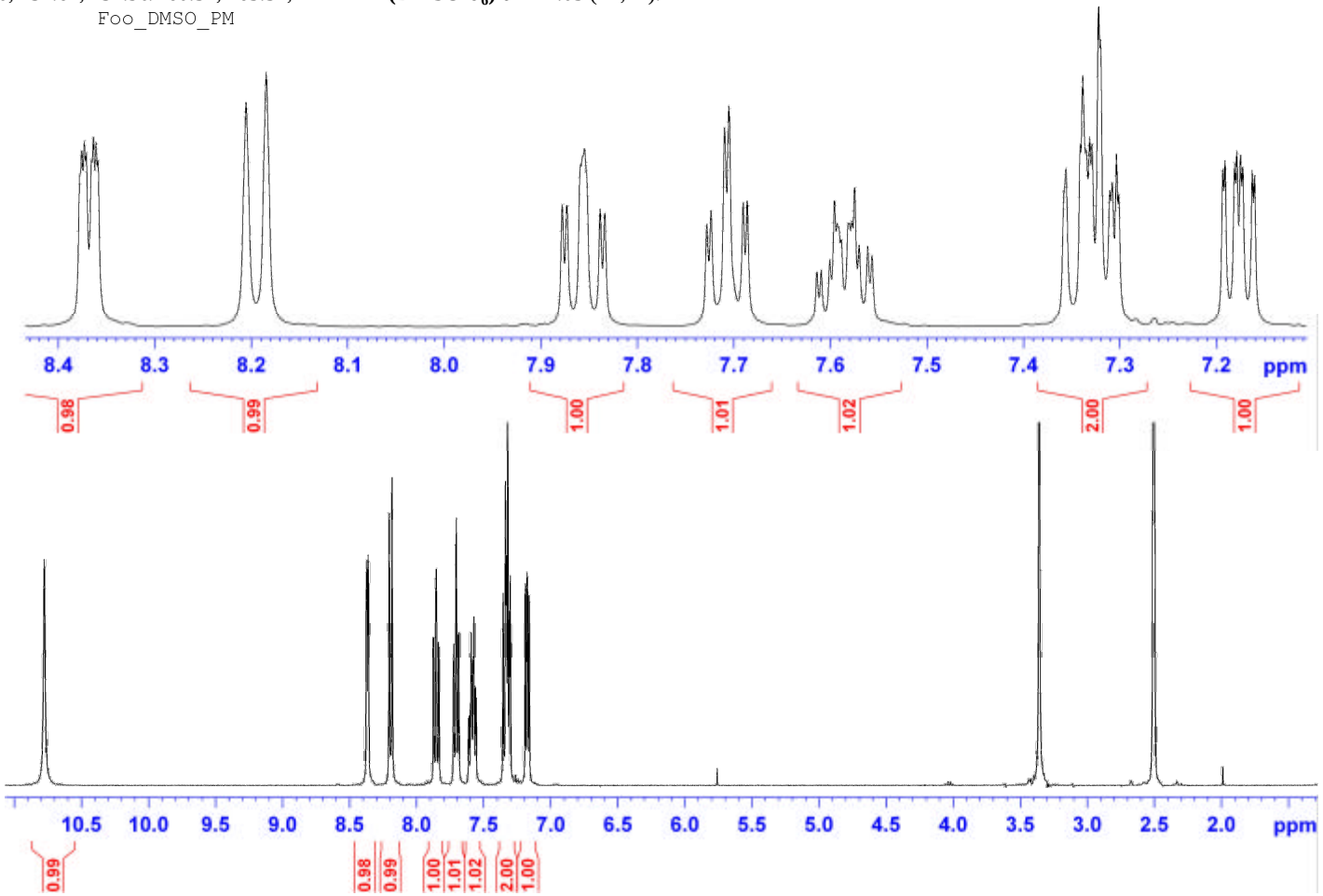

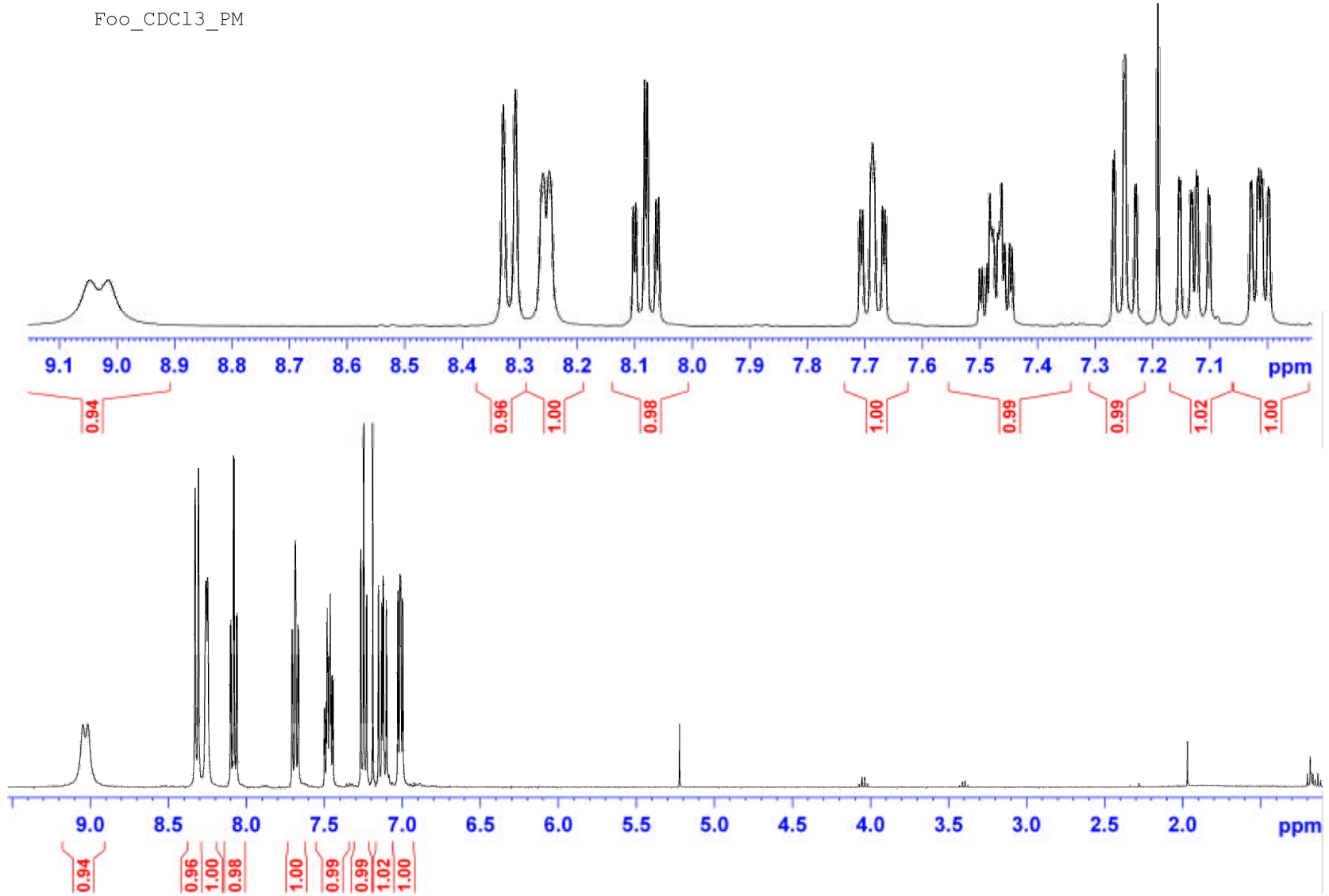
Foo_CDCl3_PM
9.1 9.0 8.9 8.8 8.7 8.6 8.5 8.4 8.3 8.2 8.1 8.0 7.9 7.8 7.7 7.6 7.5 7.4 7.3 7.2 7.1 ppm
0.94 0.96 1.00 0.98 1.00 1.00 0.99 0.99 1.02 1.00
9.0 8.5 8.0 7.5 7.0 6.5 6.0 5.5 5.0 4.5 4.0 3.5 3.0 2.5 2.0 ppm
0.94 0.96 1.00 0.98 1.00 0.99 0.99 1.02 1.00

3. IR (ATR)

3.1. Fpp

IR (ATR): 3298 (w), 3243 (w), 3166 (w), 3073 (w), 3060 (w), 3040 (w), 3029 (w), 2996 (w), 1677 (s), 1601 (s), 1587 (s), 1524 (s), 1500 (s), 1417 (s)

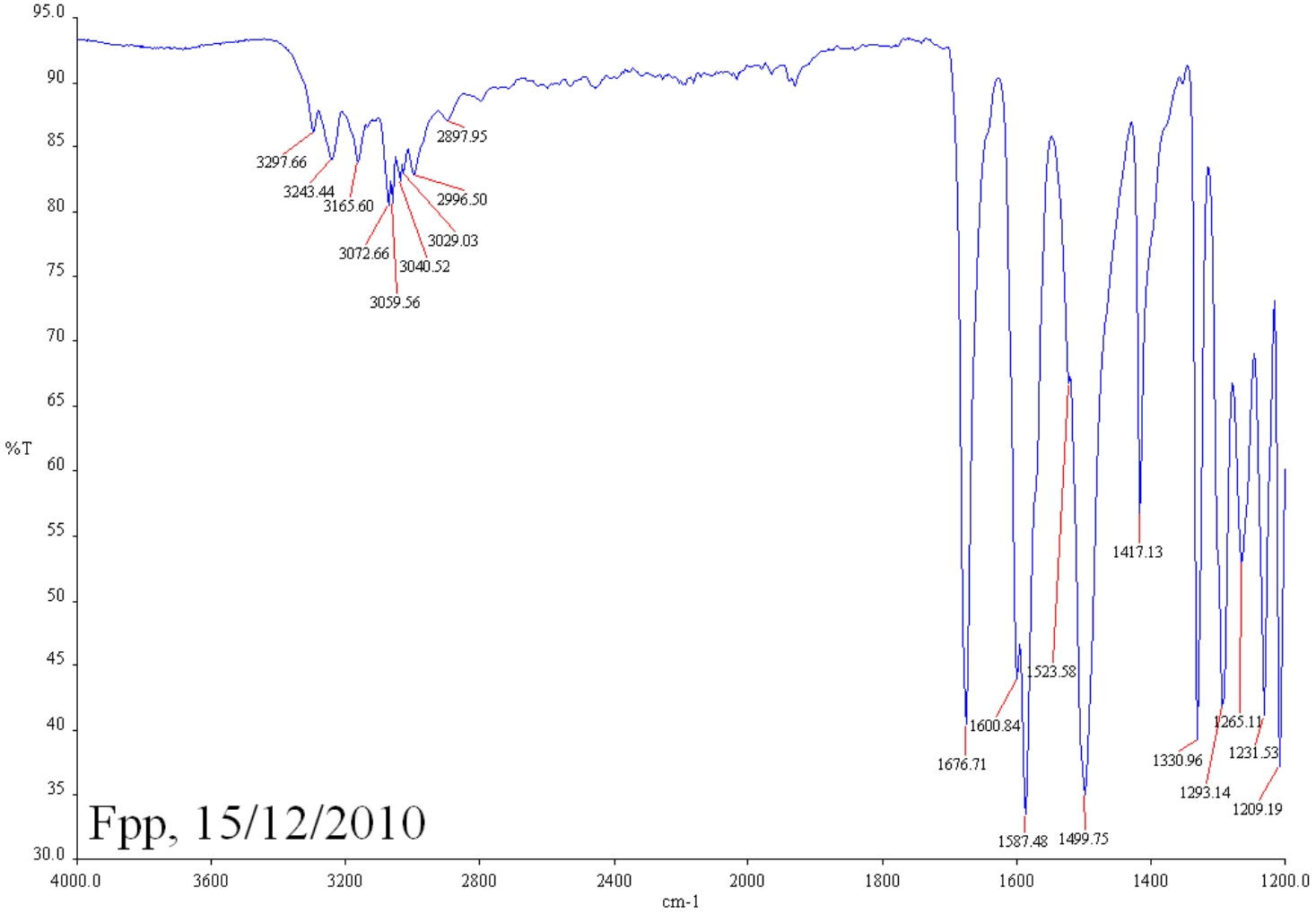

3.2. Fmp

IR (ATR): 3296 (w), 3241 (w), 3164 (w), 3068 (w), 3044 (w), 3000 (w), 2898 (w), 1680 (s), 1598 (m), 1584 (s), 1526 (w), 1506 (s), 1484 (s), 1440 (m), 1416 (m);

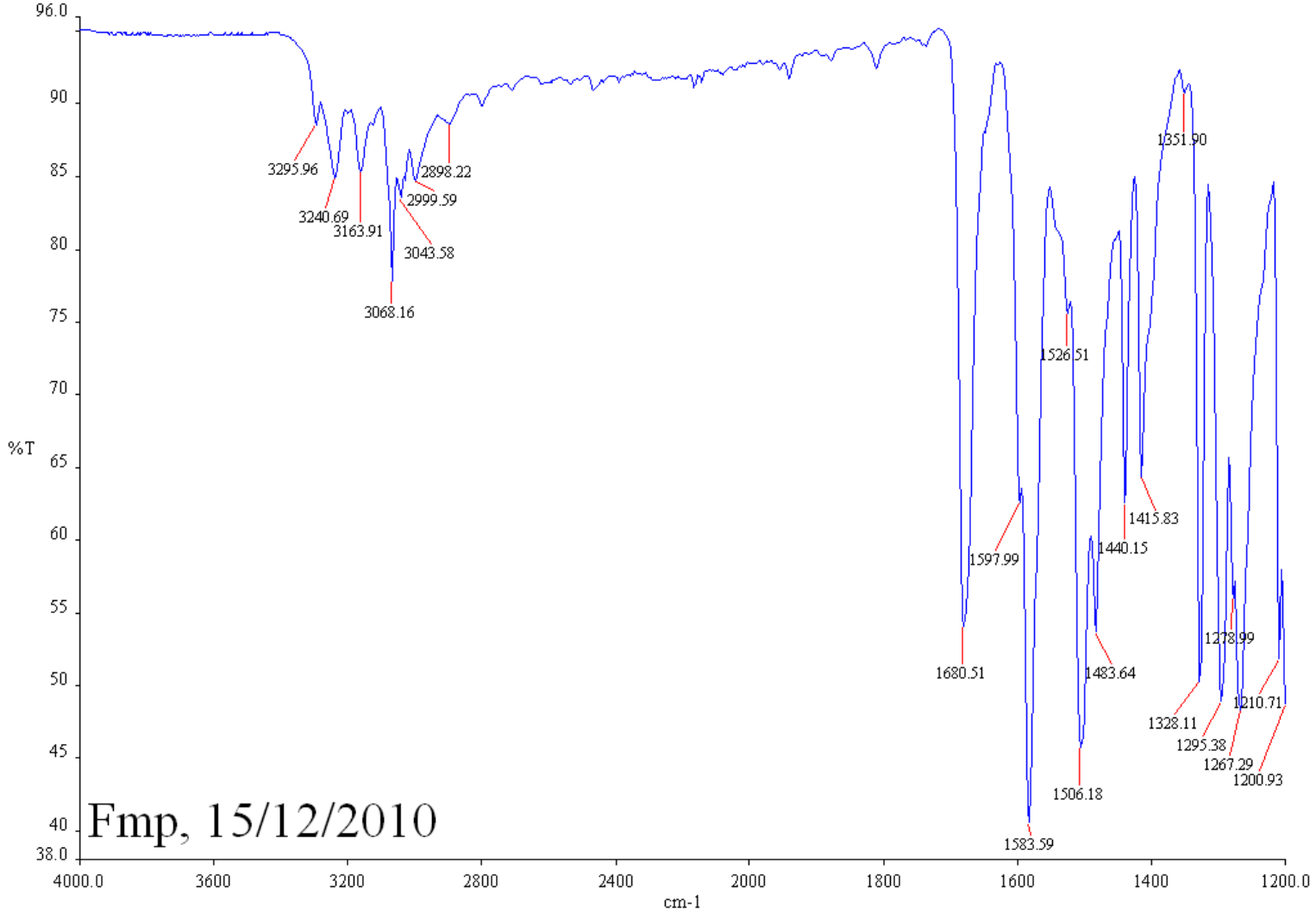

3.3. Fop

IR (ATR): 3317 (w), 3259 (w), 3175 (w), 3074 (w), 3039 (w), 3010 (w), 2906 (w), 1681 (s), 1612 (m), 1589 (s), 1509 (s), 1485 (s), 1454 (s), 1417 (m)

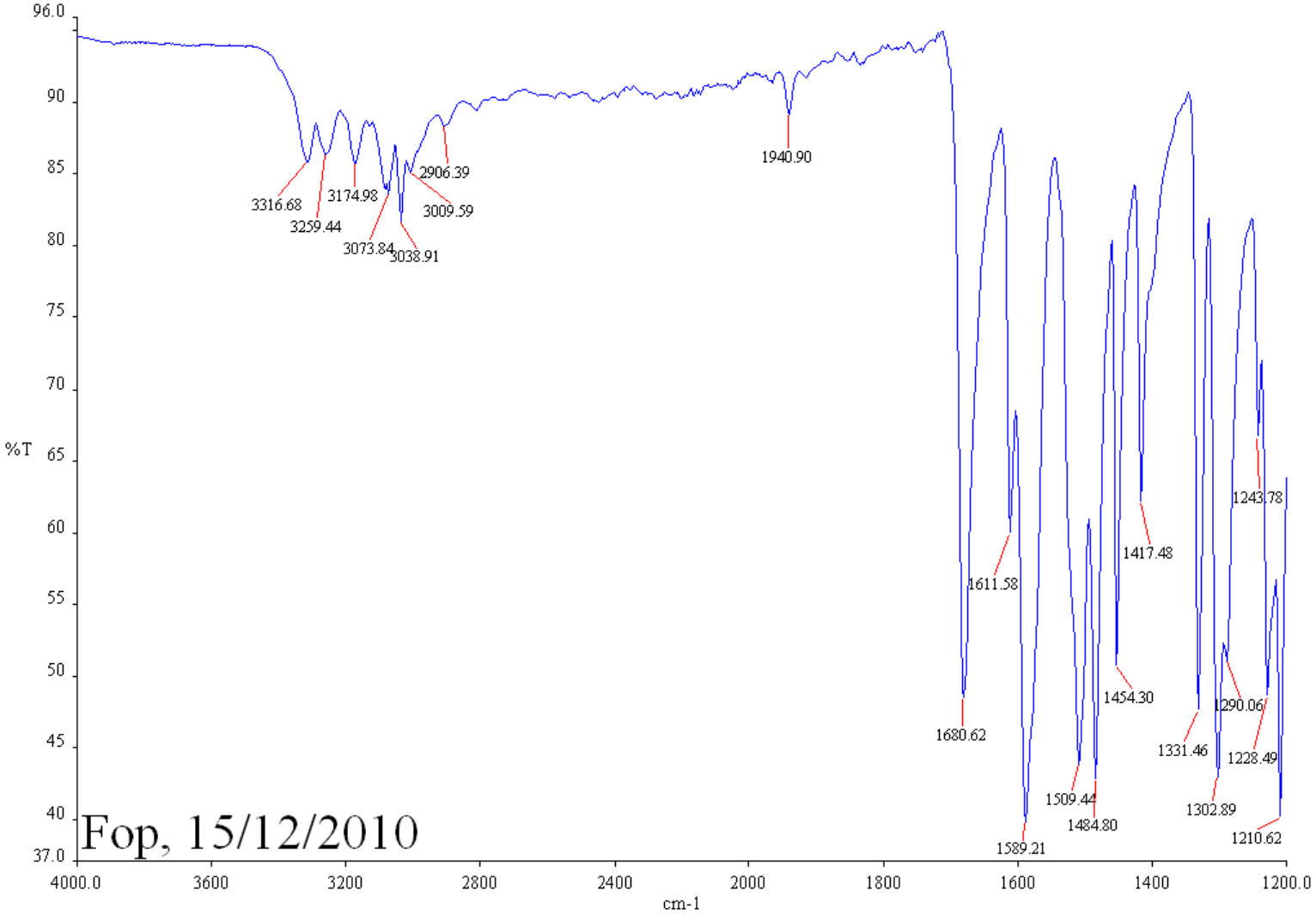

3.4. Fpm-CHF_[N-H...O=C interactions]

IR (ATR): 3324 (m), 3122 (w), 3066 (w), 3045 (w), 1682 (w), 1646 (s), 1603 (s), 1591 (m), 1527 (s), 1506 (s), 1481 (s), 1415 (m)

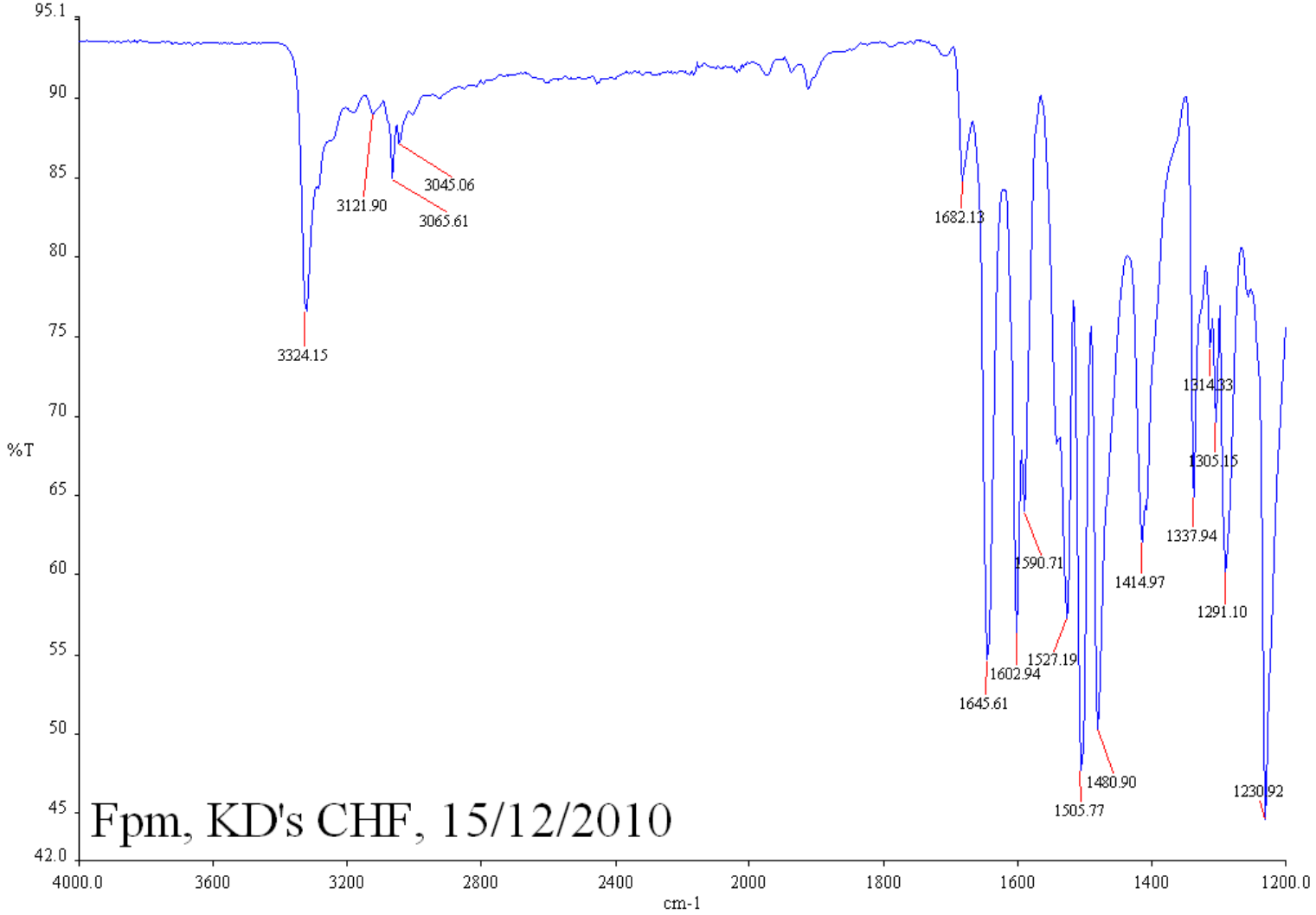

3.5. Fpm-EA [N-H...N chains]

IR (ATR): 3247 (w), 3185 (w), 3125 (w), 3106 (w), 3072 (w), 3045 (w), 3009 (w), 1681 (s), 1607 (s), 1586 (s), 1508 (s), 1475 (m), 1418 (s)

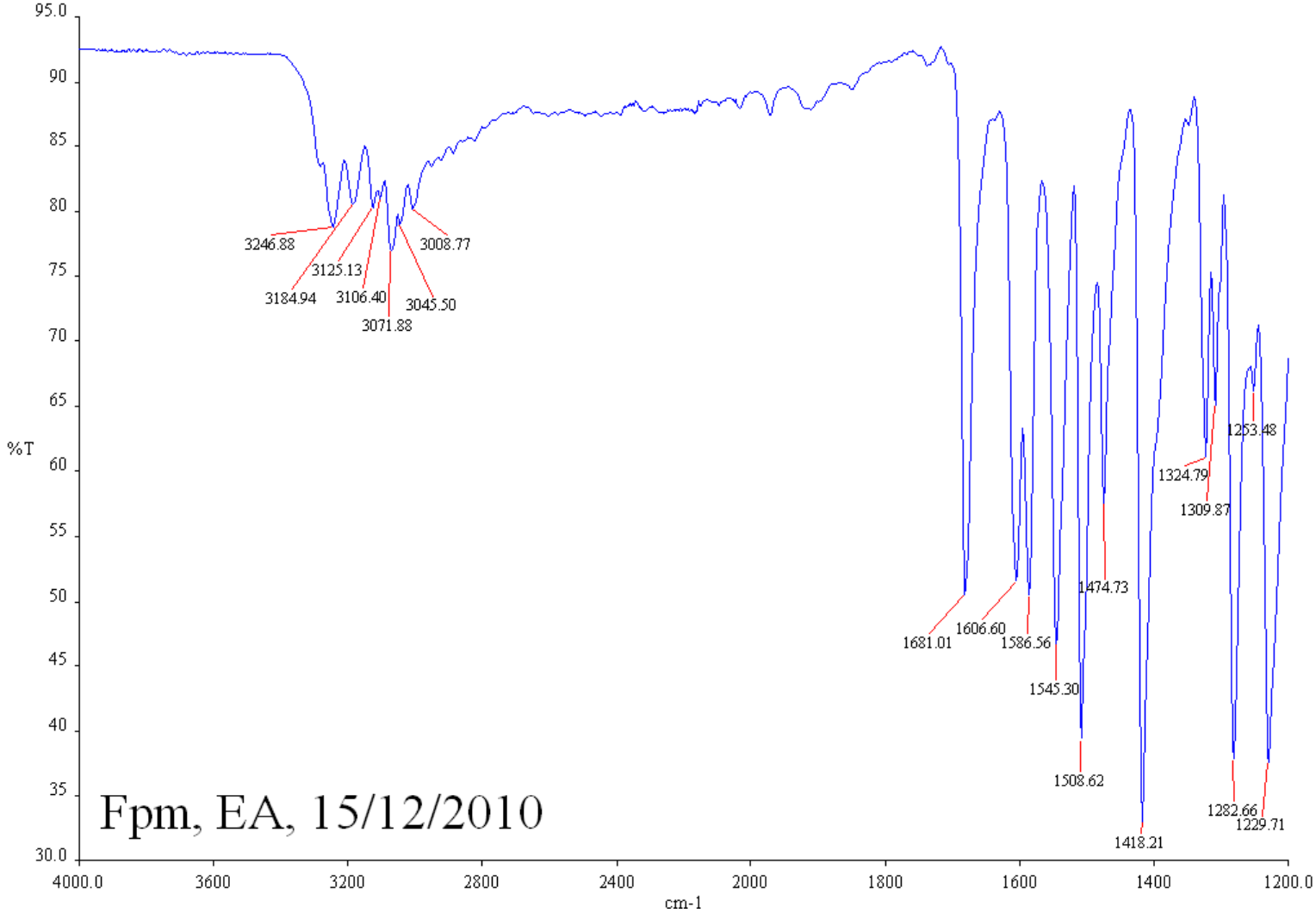

3.5. Fmm

IR (ATR): 3235 (w), 3178 (w), 3119 (w), 3068 (w), 3001 (w), 2948 (w), 2896 (w), 2837 (w), 1678 (s), 1605 (m), 1586 (s), 1548 (s), 1477 (m), 1439 (m), 1421 (s)

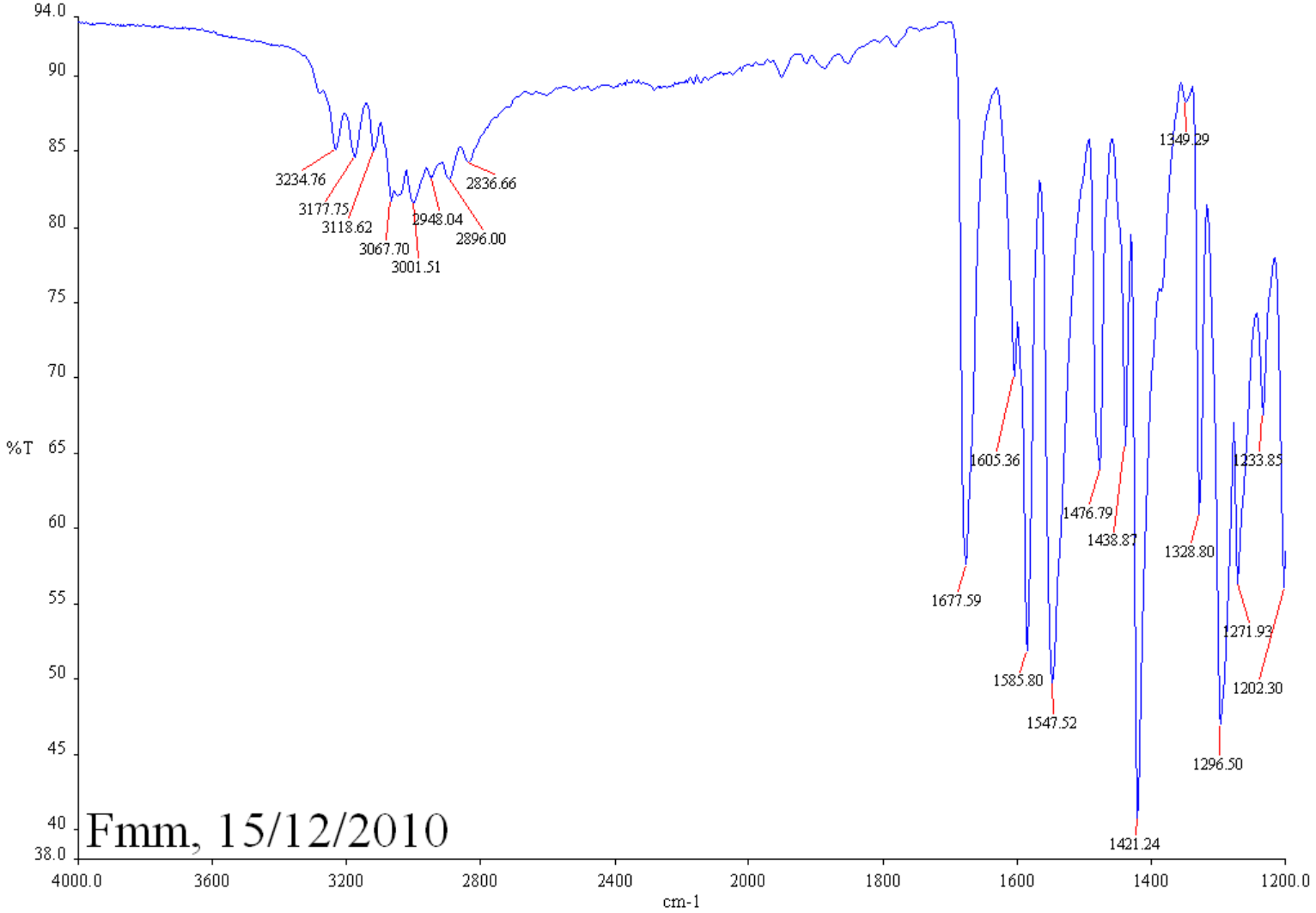

3.6. Fom

IR (ATR): 3358 (m), 3039 (w), 1665 (s), 1611 (m), 1598 (s), 1574 (w), 1537 (s), 1481 (s), 1454 (s), 1410 (s)

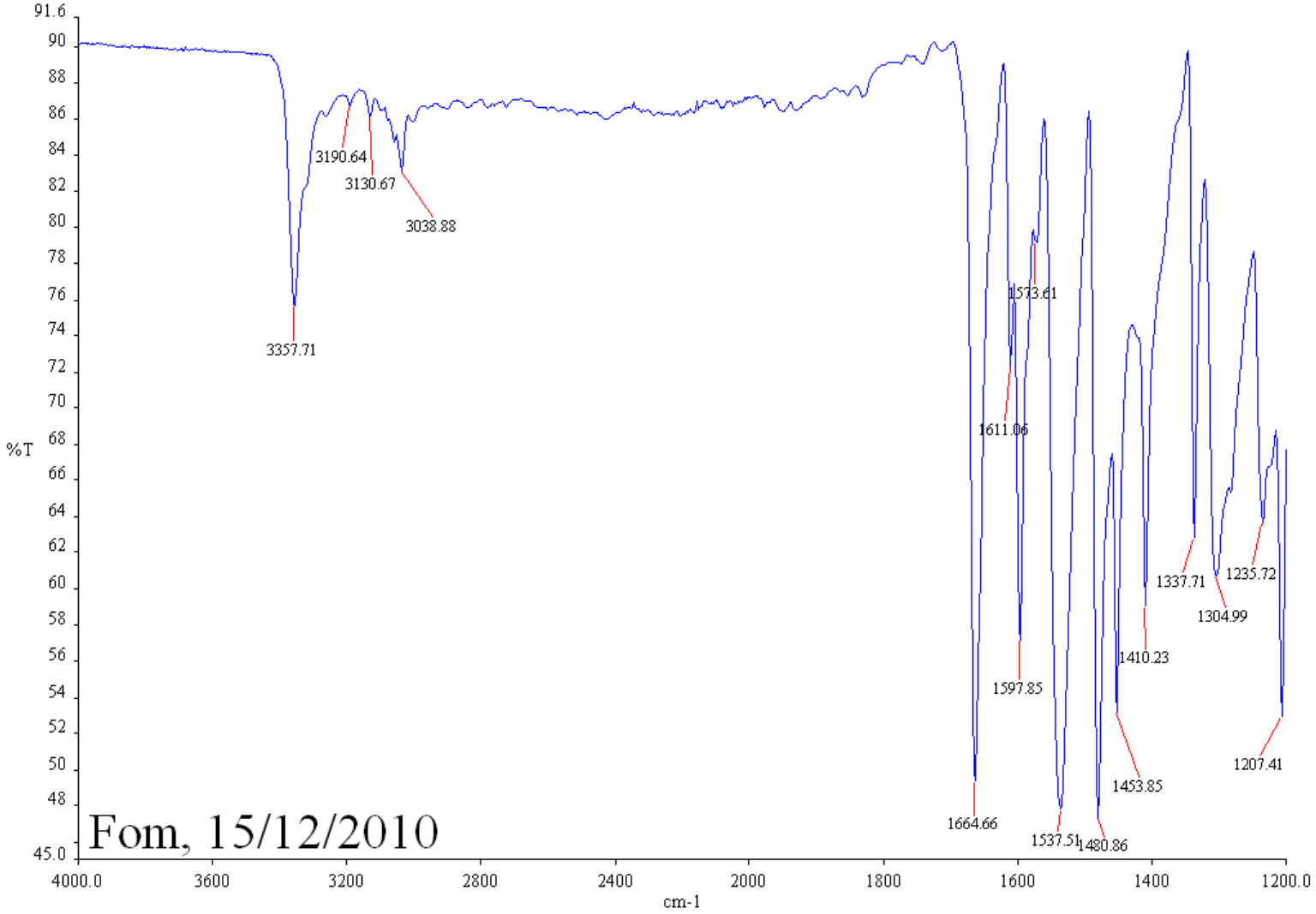

3.7. Fpo

IR (ATR): 3170 (w), 3115 (w), 3083 (w), 2993 (w), 2956 (w), 2927 (w), 1673 (s), 1600 (m), 1581 (s), 1534 (m), 1503 (s), 1463 (m), 1436 (s), 1411 (m)

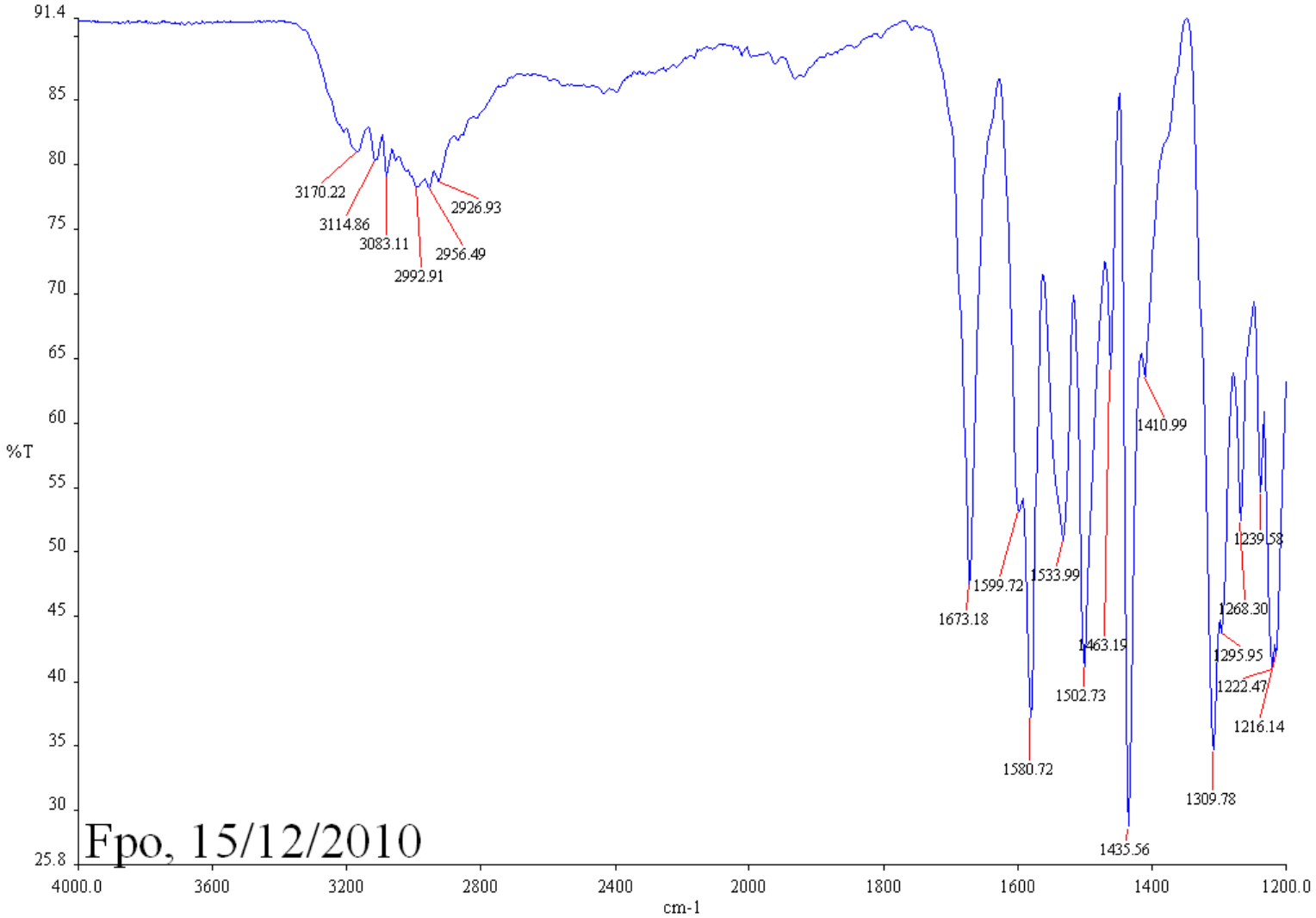

3.8. Fmo

IR (ATR): 3169 (w), 3108 (w), 3076 (w), 2994 (w), 1679 (s), 1579 (s), 1522 (s), 1481 (s), 1464 (m), 1433 (s)

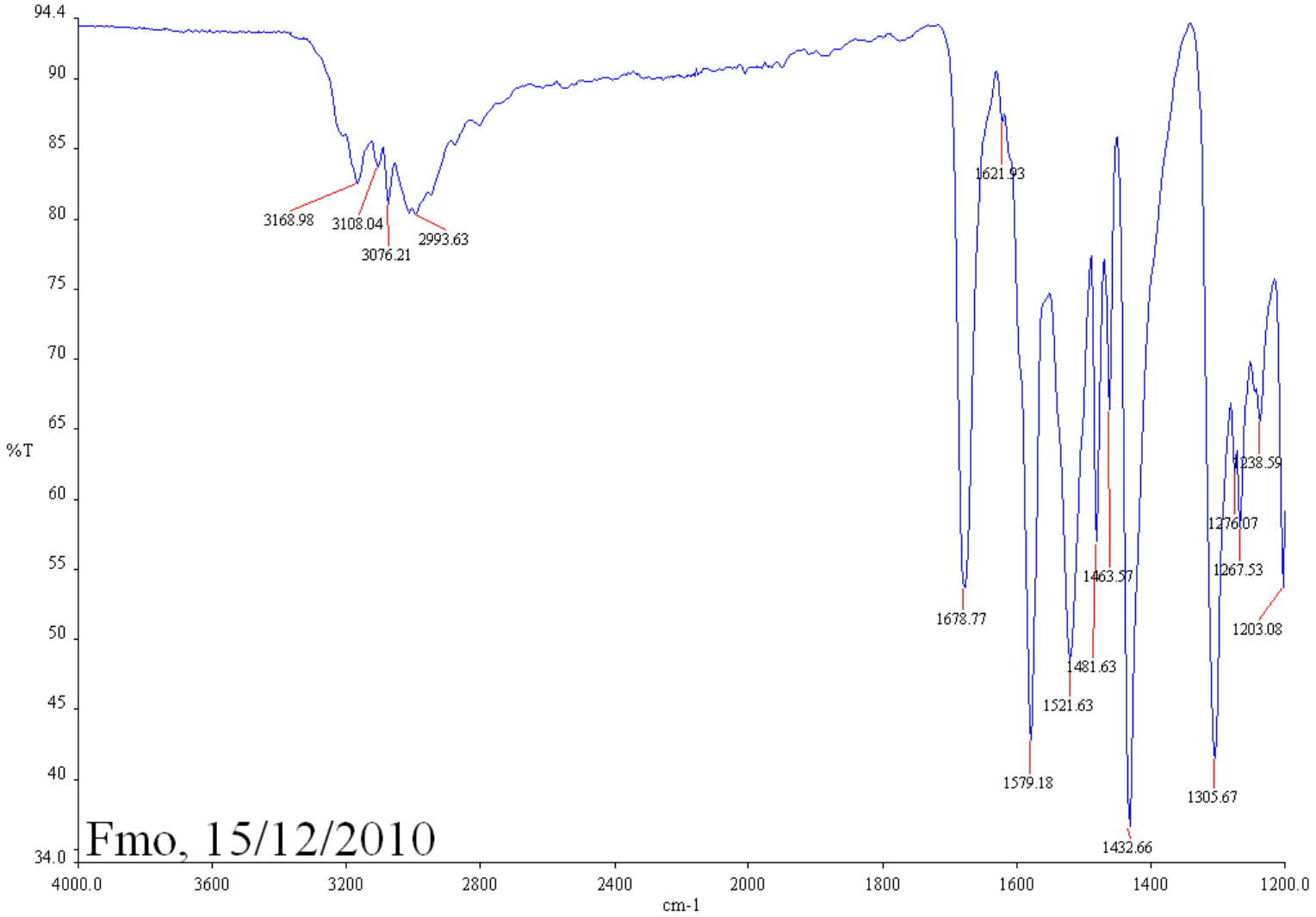

3.9. Foo

IR (ATR): 3178 (w), 3112 (w), 3015 (w), 1685 (s), 1612 (m), 1599 (m), 1579 (s), 1536 (s), 1487 (s), 1464 (m), 1454 (s), 1434 (s)

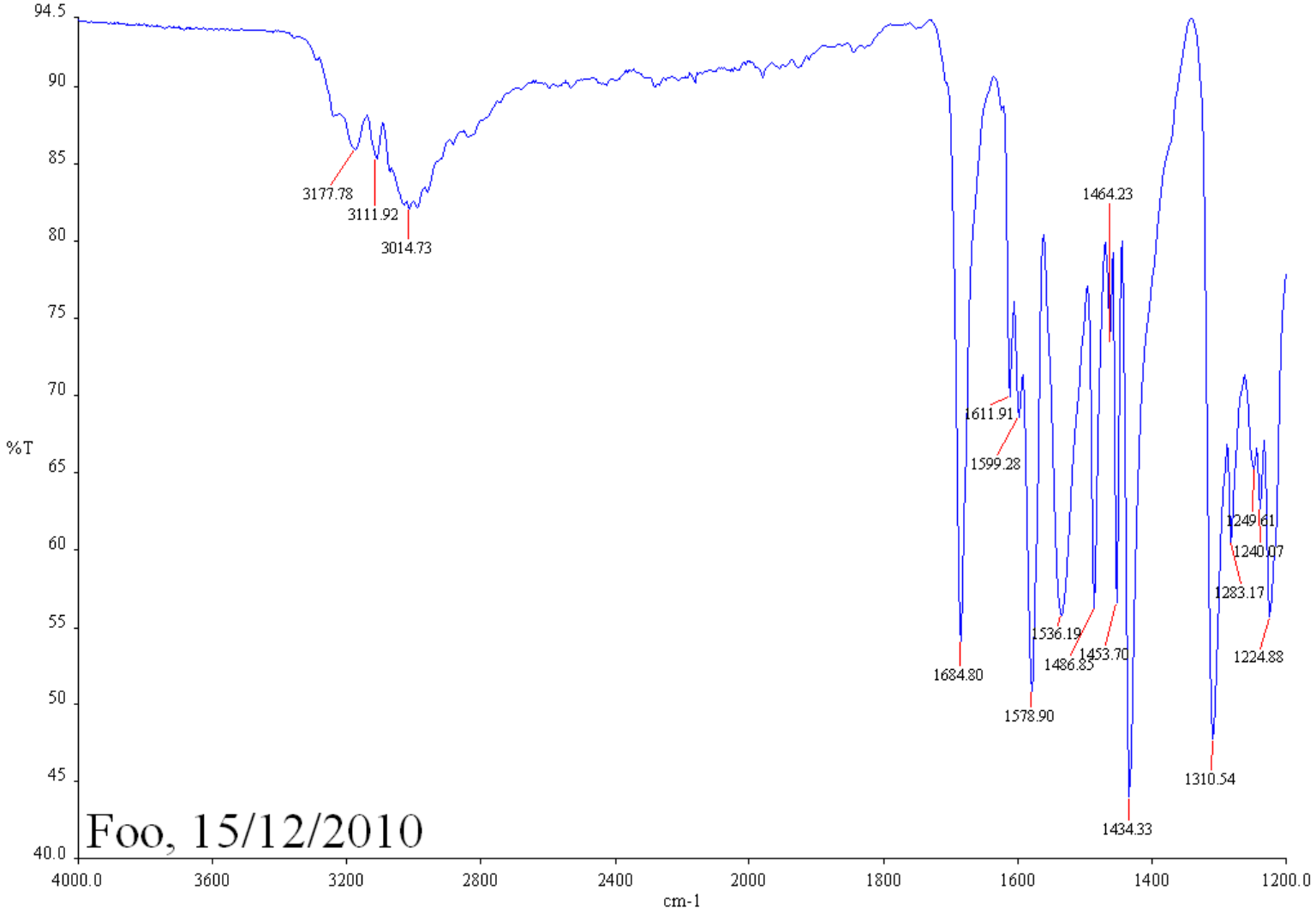

4. Crystallographic details for all Fxx isomers.

4.1. Table 2a. Experimental details for all eleven Fxp/Fxm/Fxo isomers

For all structures: $C_{12}H_9N_2OF$, M_r = 212.25. Experiments were carried out at 294 K with Mo *K*α radiation using a Xcalibur, Sapphire3, Gemini Ultra diffractometer. H atoms were treated by a mixture of independent and constrained refinement (N-H H atoms were refined with isotropic displacement parameters). Isomer name with **CSD code** below.

	Fpp 865570 [10-124]	**Fmp** 865571 10-126	**Fop** 865572 10-125	**Fpm_O** 865573 10-127	**Fpm_N** 865574 10-121	**Fmm** 865575 10-122
Crystal data						
Crystal system, space group	Monoclinic $P2_1/c$	Monoclinic $P2_1/c$	Monoclinic $P2_1/c$	Monoclinic $P2_1/n$	Monoclinic $P2_1/n$	Orthorhombic $Pca2_1$
a, *b*, *c* (Å)	5.67770(10) 11.4769(2), 15.5289(3)	5.79610(10), 11.3050(2), 15.2384(2)	6.03880(10), 11.2502(2), 14.9265(3)	13.9411(3), 5.20400(10), 15.0752(3)	3.9077(2), 24.2444(12), 10.7012(5)	11.3020(3), 11.8371(3), 7.6218(2)
α, β, γ (°)	90.00, 95.974(2), 90.00	90.00, 94.2380(10), 90.00	90.00, 95.310(2), 90.00	90.00, 114.812(3), 90.00	90.00, 95.181(5), 90.00	90.00, 90.00, 90.00
V (Å^3)	1006.40(3)	995.76(3)	1009.72(3)	992.74(3)	1009.69(9)	1019.67(5)
Z	4	4	4	4	4	4
μ (mm^{-1})	0.106	0.107	0.106	0.108	0.106	0.105
Crystal size (mm)	0.19 ×0.25 ×0.39	0.37× 0.34 ×0.19	0.45× 0.30 ×0.08	0.51× 0.49 ×0.32	0.24×0.05 ×0.03	0.38×0.10 ×0.08
Data collection						
Absorption correction	Analytical (ABSFAC. Clark & Reid, 1998)	Analytical (ABSFAC. Clark & Reid, 1998)	Analytical (ABSFAC. Clark & Reid, 1998)	Analytical (ABSFAC. Clark & Reid, 1998)	Analytical (ABSFAC. Clark & Reid, 1998)	Analytical (ABSFAC. Clark & Reid, 1998)
T_{min}, T_{max}	0.9598, 0.9801	0.9614, 0.9799	0.9540, 0.9916	0.9472, 0.9664	0.9751, 0.9968	0.9613, 0.9917
No. of measured, independent and observed reflns	7351, 2216, 1979, 2σ(I)	7728, 2202, 1988, 2σ(I)	7133, 2256, 1914, 2σ(I)	8861, 2624, 2338, 2σ(I)	6537, 2162, 1154, 2σ(I)	7366, 1239, 981, 2σ(I)
R_{int}	0.0126	0.0115	0.0160	0.0117	0.0488	0.0205
Refinement						
$R[F^2 > 2\sigma(F^2)]$, $wR(F^2)$, *S*	0.0337, 0.0898, 1.043	0.0341, 0.0922, 1.050	0.0374, 0.1030, 1.020	0.0415, 0.1135, 1.032	0.0527, 0.1199, 0.960	0.0330, 0.0836, 1.023
No of reflections	2216	2202	2256	2624	2162	1239
No. of parameter	150	150	150	150	149	149
No. of restraints	0	0	0	0	0	0
$\Delta\rangle_{max}$, $\Delta\rangle_{min}$ (e Å^{-3})	0.20, -0.14	0.24, -0.17	0.23, -0.16	0.25, -0.19	0.16, -0.16	0.15, -0.15

	Fom_O 865576 11-009	**Fom_F** 865577 11-061	**Fpo** 865578 10-123	**Fmo** 865579 11-003	**Foo** 865590 10-128
Crystal data					
Crystal system, space group	Monoclinic $P2_1$	Monoclinic $P2_1/n$	Orthorhombic *Pbcn*	Triclinic, *P* ?	Triclinic, *P* ?
a, *b*, *c* (Å)	16.2051(4) 5.22390(10) 35.8162(9)	5.4788(2), 8.8223(4), 20.4414(7)	24.3381(4), 7.93340(10), 10.8791(2)	10.4219(4), 10.7183(4), 11.0188(3)	9.7560(4), 10.7699(5), 11.9694(2)
α, β, γ (°)	90.00 98.405(3) 90.00	90.00, 92.150(4) 90.00	90.00 90.00 90.00	102.286(3) 97.356(3) 117.074(4)	64.412(4) 68.453(4) 86.091(4)
V (Å^3)	2999.41(12)	987.35(7)	2100.58(6)	1034.49(8)	1048.88(7)
Z	12	4	8	4	4
μ (mm^{-1})	0.893	0.108	0.102	0.103	0.102
Crystal size (mm)	0.47×0.23× 0.16	0.49×0.25 ×0.12	0.58×0.53 ×0.17	0.44×0.35 ×0.28	0.42×0.35 ×0.28
Data collection					
Absorption correction	Analytical (ABSFAC. Clark & Reid, 1998)	Analytical (ABSFAC. Clark & Reid, 1998)	Analytical (ABSFAC. Clark & Reid, 1998)	Analytical (ABSFAC. Clark & Reid, 1998)	Analytical (ABSFAC. Clark & Reid, 1998)
T_{min}, T_{max}	0.6789 0.8703	0.9489, 0.9871	0.9434, 0.9829	0.9560, 0.9717	0.9585, 0.9721
No. of measured, independent and observed reflns	13035, 5835, 5064, 2σ(I)	7439, 2178, 1599, 2σ(I)	14121, 2254, 1829, 2σ(I)	14851, 4555, 3732, 2σ(I)	9959, 5437, 4377, 2σ(I)
R_{int}	0.0262	0.0266	0.0242	0.0161	0.0119
Refinement					
$R[F^2 > 2\sigma(F^2)]$, $wR(F^2)$, *S*	0.0594, 0.1763, 1.018	0.0437, 0.1217, 1.046	0.0422, 0.1131, 1.037	0.0464, 0.1244, 1.034	0.0437, 0.1141, 1.037
No. of reflections	5835	2178	2254	4555	5437
No. of parameters	1315	149	150	298	298
No. of restraints	638	0	0	0	0
$\Delta\rangle_{max}$, $\Delta\rangle_{min}$ (e Å^{-3})	0.16, -0.19	0.14, -0.18	0.14, -0.17	0.29, -0.25	0.31, -0.23

Computer programs: CrysAlisPro, Oxford Diffraction Ltd., Version 1.171.33.55 (release 05-01-2010 CrysAlis171 .NET) (compiled Jan 5 2010,16:28:46), *SHELXS97* (Sheldrick, 2008), *SHELXL97* (Sheldrick, 2008) and SORTX (McArdle, 1995), *PLATON* (Spek, 2009), *SHELXL97*.

The **Fxx** CCDC reference codes are **865570** to **865580**.

4.2 Table 2b. Selected hydrogen-bond parameters for the nine Fxx isomers.

D—H···*A*	*D*—H (Å)	H···*A* (Å)	*D*···*A* (Å)	*D*—H···*A* (°)
Fpp_[10-124]				
N1-H1···N24^{i}	0.848(16)	2.335(17)	3.0581(15)	143.5(14)
Fmp_[10-126]				
N1-H1···N24^{i}	0.852(15)	2.333(16)	3.0786(14)	146.5(13)
Fop_[10-125]				
N1-H1···N24^{i}	0.862(18)	2.356(18)	3.0587(16)	138.9(15)
N1-H1···F12	0.862(18)	2.332(17)	2.7491(13)	110.0(13)
Fpm_O_[10-127]				
N1-H1···O1^{ii}	0.859(17)	2.221(17)	3.0575(13)	164.6(14)
C26-H26···O1	0.93	2.45	2.8987(15)	109
C15-H15···N23^{iii}	0.93	2.68	3.5891(17)	164
C24-H24···N23^{iv}	0.93	2.76	3.5663(16)	146
Fpm_N_[10-121]				
N1-H1···N23^{v}	0.84(3)	2.32(3)	3.151(3)	167(2)
C16-H16···N23^{v}	0.93	2.60	3.404(3)	146
C22-H22···O1	0.93	2.21	2.828(3)	123
C26-H26···N23^{v}	0.93	2.60	3.390(3)	144
Fmm_[10-122]				
N1-H1···N23^{vi}	0.77(3)	2.31(3)	3.077(3)	176(3)
C22-H22···O1	0.93	2.22	2.829(3)	123
C14-H14···O1^{vii}	0.93	2.77	3.619(3)	152
C24-H24···O1^{viii}	0.93	2.74	3.343(3)	123
C25-H25···F13^{ix}	0.93	2.66	3.364(3)	133
Fom_O_[11-009] Intramolecular data for molecules A to D only				
N1A-H1A...F12A	0.86	2.26	2.766(5)	118
N1B-H1B...F12B	0.86	2.19	2.720(5)	119
N1C-H1C...F12C	0.86	2.20	2.727(5)	119
N1D-H1D...F12D	0.86	2.22	2.723(5)	117
Molecules aggregate in the b-axis (010) direction via N-H...O=C interactions in **Fom_O**				

Fom_F_[11-061]				
N1-H1...O1^{x}	0.850(17)	2.641(17)	3.3321(17)	139.3(15)
C14-H14...N23^{xi}	0.93	2.70	3.427(2)	135
N1-H1...F12	0.850(17)	2.074(17)	2.7315(16)	133.7(15)
C16-H16...O1	0.93	2.46	2.7777(19)	100
C22-H22...O1	0.93	2.30	2.867(2)	119
Fpo_[10-123]				
N1-H1···N22^{xii}	0.883(17)	2.186(17)	3.0608(18)	171.0(15)
C12-H12···F14^{xiii}	0.93	2.56	3.443(2)	160
C12-H12···O1	0.93	2.61	2.846(2)	95
C15-H15···C12^{xiv}	0.93	2.83	3.757(2)	178
C16-H16···O1^{xiv}	0.93	2.59	3.266(2)	130
C25-H25···O1^{xv}	0.93	2.66	3.498(2)	150
Fmo_[11-003]				
N1A-H1A···N22B	0.876(18)	2.199(18)	3.0721(17)	174.1(15)
N1B-H1B···N22A	0.870(17)	2.183(18)	3.0502(18)	174.9(15)
C26A-H26A···O1A	0.93	2.30	2.844(2)	117
C26B-H26B···O1B	0.93	2.25	2.836(3)	120
C25A-H25A...O1B^{xvi}	0.93	2.33	3.235(2)	163
Foo_[10-128]				
N1A-H1A...N22B	0.871(16)	2.177(16)	3.0460(14)	175.7(14)
N1B-H1B...N22A	0.870(16)	2.193(16)	3.0408(15)	164.8(14)
N1A-H1A...F12A	0.871(16)	2.960(15)	3.0773(15)	89.4(10)
N1B-H1B...F12B	0.870(16)	2.487(16)	2.7981(15)	101.8(12)

Symmetry code(s):

i=[-x+1, y+1/2, -z+1/2]; ii=[x, y+1, z]; iii=[-x+1, -y+1, -z]; iv= [-x+1/2, y-1/2, -z+1/2]; v= [x-1/2, -y+1/2, z-1/2]; vi= [x+1/2, -y+1, z]; vii= [x+1/2, -y, z]; viii= [-x, -y+1, z-1/2]; ix= [-x+1/2, y+1, z-1/2]; x= [x+1, y, z]; xi= [x+1/2, -y+1/2, z+1/2]; xii= [-x, y, -z+1/2]; xiii= [-x+1/2, -y+3/2, z+1/2]; xiv= [x, -y+1, z-1/2]; xv= [-x, y, -z+3/2], xvi= [x, y+1, z].

Fom_O is an unusual structure

The **Fom_O** polymorph crystallises from a range of solvents in space group $P2_1$ with Z'=6. The structure solves easily in $P2_1$ using common structure solution programs and default settings BUT even at this stage it is obvious that there is considerable disorder present. On refinement the **Fom_O** structure is revealed to be completely disordered with the six individual molecules having varying levels of disorder from four molecules with a minor component of disorder (~10%) and two being completely disordered with 50% occupancy for each site. The systematic absences suggest $P2_1$ or $P2_1/m$ and it readily solves in P21. There is a suggested systematic weakness for h = 3n, 6n.
Refinement incorporating disorder models brought the two molecules to 0.87:0.13, two to 0.83:0.17 and E/H, F/G to 50:50 occupancy with esd's of 0.005 on the occupancy. These were fixed in the final refinement cycles. The several Alert errors stem from the disorder process. Final refinement converged at 6%.

5. *Ab initio* calculation results

5.1. Geometry parameters for Fxx isomers optimised using different basis sets

	6-311++G**			6-311++G			6-311G**		
	α/°	β/°	δ/°	α/°	β/°	δ/°	α/°	β/°	δ/°
Fpp	-24.45	-5.33	-3.10	-25.75	-3.74	-4.69	-22.27	-4.24	-2.87
Fmp	-24.95	-4.70	-2.85	151.63	-3.69	-4.24	-23.52	-4.24	-2.37
Fop	-0.03	0.01	0.03	0.00	0.00	0.00	0.00	0.00	0.00
Fpm	-24.27	-5.67	-2.51	-25.54	-3.45	-4.30	-22.07	-4.14	-2.34
Fmm	-24.62	-4.79	-2.29	151.90	-3.68	-3.84	-23.20	-4.15	-1.84
Fom	0.01	0.00	-0.02	-0.05	0.02	-0.02	0.02	0.01	-0.03
Fpo	-21.73	-3.44	-2.66	-22.36	-2.06	-3.86	-19.05	-3.68	-2.10
Fmo	-22.08	-2.96	-2.55	-21.95	-1.75	-3.68	-19.69	-3.34	-2.09
Foo	-0.01	0.00	0.00	-0.02	-0.02	0.04	-0.01	0.00	0.00

5.2. Energy results

5.2.1. Table 3. Optimised in *gas phase* (CBS-QB3)

	E_{SCF}	δE_{SCF}	E_0	δE_0	E	δE	G	δG
Fpp	-743.1102	-14.18	-746.1022	-3.84	-746.0895	-3.90	-746.1431	-3.70
Fmp	-743.1089	-10.84	-746.1023	-4.09	-746.0896	-4.17	-746.1431	-3.77
Fop	-743.1091	-11.36	-746.1028	-5.59	-746.0902	-5.82	-746.1437	-5.37
Fpm	-743.1060	-3.12	-746.1007	0.00	-746.0880	0.00	-746.1417	0.00
Fmm	-743.1048	0.00	-746.1008	-0.35	-746.0881	-0.38	-746.1418	-0.22
Fom	-743.1049	-0.35	-746.1013	-1.64	-746.0887	-1.80	-746.1424	-1.74
Fpo	-743.1196	-38.81	-746.1109	-26.79	-746.0983	-27.02	-746.1518	-26.44
Fmo	-743.1183	-35.44	-746.1110	-27.06	-746.0984	-27.32	-746.1518	-26.49
Foo	-743.1171	-32.36	-746.1101	-24.75	-746.0976	-25.18	-746.1509	-24.26

5.2.2. Table 4. Optimisation in CH_2Cl_2 (PCM-SMD/CBS-QB3)

	E_{SCF}	δE_{SCF}	E_0	δE_0	E	δE	G	δG
Fpp	-743.1380	-26.35	-746.1269	-11.73	-746.1143	-11.89	-746.1674	-11.14
Fmp	-743.1365	-22.38	-746.1272	-12.64	-746.1145	-12.50	-746.1681	-12.92
Fop	-743.1331	-13.56	-746.1246	-5.69	-746.1127	-7.93	-746.1635	-0.92
Fpm	-743.1326	-12.17	-746.1246	-5.68	-746.1119	-5.78	-746.1652	-5.22
Fmm	-743.1312	-8.51	-746.1249	-6.67	-746.1122	-6.43	-746.1660	-7.48
Fom	-743.1279	0.00	-746.1224	0.00	-746.1097	0.00	-746.1632	0.00
Fpo	-743.1445	-43.50	-746.1334	-29.00	-746.1208	-29.06	-746.1744	-29.50
Fmo	-743.1430	-39.56	-746.1339	-30.20	-746.1211	-29.75	-746.1751	-31.34
Foo	-743.1395	-30.25	-746.1305	-21.41	-746.1180	-21.73	-746.1709	-20.24

5.2.3. Table 5. Optimisation in H_2O (PCM-SMD/CBS-QB3)

	E_{SCF}	δE_{SCF}	E_0	δE_0	E	δE	G	δG
Fpp	-743.1328	-28.89	-746.12023	-15.46	-746.1075	-15.21	-746.1613	-17.02
Fmp	-743.1314	-25.31	-746.12000	-14.84	-746.1074	-14.75	-746.1610	-16.35
Fop	-743.1269	-13.58	-746.11668	-6.15	-746.1049	-8.18	-746.1560	-3.10
Fpm	-743.1273	-14.67	-746.11785	-9.20	-746.1051	-8.87	-746.1590	-11.06
Fmm	-743.1262	-11.57	-746.11764	-8.66	-746.1050	-8.55	-746.1584	-9.45
Fom	-743.1218	0.00	-746.11434	0.00	-746.1017	0.00	-746.1548	0.00
Fpo	-743.1363	-38.19	-746.12392	-25.13	-746.1112	-24.82	-746.1651	-27.11
Fmo	-743.1348	-34.38	-746.12371	-24.59	-746.1110	-24.32	-746.1650	-26.80
Foo	-743.1305	-22.98	-746.12008	-15.07	-746.1075	-15.14	-746.1606	-15.18

The tables present absolute values of electronic (E_{SCF}), zero point (E_0), energy (E) and Gibbs free energy (G) for the nine **Fxx** isomers expressed in Hartrees (E_h). The relative energies (**Fpm, Fmm** or **Fom** is taken as basis point) are shown in columns with suffix δ, and are expressed in $kJ.mol^{-1}$.

5.2.4. Table 6. Comparison of energies in different media

	gas phase vs. CH_2CH_2				*gas phase vs.* H_2O				CH_2Cl_2 *vs.* H_2O				$logK_{D/W}$
	ΔE_{SCF}	ΔE_0	ΔE	ΔG_{solv}	ΔE_{SCF}	ΔE_0	ΔE	ΔG_{solv}	ΔE_{SCF}	ΔE_0	ΔE	ΔG_{solv}	
Fpp	-72.97	-64.80	-65.11	-63.81	-59.25	-47.40	-47.45	-47.66	-13.72	-17.40	-17.66	-16.15	2.83
Fmp	-72.34	-65.46	-65.45	-65.52	-59.01	-46.53	-46.71	-46.92	-13.33	-18.93	-18.74	-18.60	3.26
Fop	-63.00	-57.01	-59.23	-51.92	-46.75	-36.34	-38.50	-32.07	-16.24	-20.67	-20.74	-19.85	3.48
Fpm	-69.85	-62.59	-62.90	-61.59	-56.09	-44.98	-45.00	-45.40	-13.76	-17.61	-17.90	-16.19	2.84
Fmm	-69.31	-63.22	-63.17	-63.63	-56.10	-44.09	-44.30	-43.58	-13.21	-19.13	-18.87	-20.05	3.51
Fom	-60.45	-55.27	-55.32	-54.63	-44.19	-34.14	-34.33	-32.60	-16.26	-21.12	-20.99	-22.03	3.86
Fpo	-65.48	-59.12	-59.17	-59.43	-43.91	-34.13	-33.94	-35.01	-21.57	-24.99	-25.23	-24.42	4.28
Fmo	-64.91	-60.05	-59.55	-61.22	-43.47	-33.31	-33.13	-34.65	-21.45	-26.74	-26.42	-26.57	4.65
Foo	-58.69	-53.58	-53.67	-52.35	-35.16	-26.10	-26.09	-25.26	-23.53	-27.47	-27.58	-27.10	4.75

Comment on energy calculations:

The energy results show that generally speaking the most stable are the **Fxo** compounds, and similarly to the **Mxx** isomer grid where the **Mxo** compounds were the most stable. The **Fxo** compounds are at least 20 kJ.mol-1 lower in energy in the *gas phase* than the rest of the isomers. The strong stabilisation comes from pyridine N atom moving into the *ortho* position. This causes delocalisation across both the *ortho*-pyridine ring and the amide linkage group, and, as seen in the modelled as well as in the solid state structures of the **Fxo** and the **Mxo** compounds, consequential co-planarity of the *ortho*-pyridine ring and the amide linkage group.

The least stable triad is the **Fxm**. In the **Mxx** isomer grid the most unstable isomer was **Mom**. However, due to the additional stabilisation from the intermolecular N-H…F hydrogen bond the most unstable isomer in *gas phase* is not **Fom** but **Fmm**. Alternatively, the hydrogen bonding is disrupted in the solvated form and therefore, **Fom** is the most unstable isomer in solvent.

The obtained theoretical values of **?** G_{solv} in CH_2Cl_2 and H_2O, including theoretical $logK_{D/W}$ are consistent with experimental observations and with no unexpected values. The **Fxo** series are expected to be the least soluble in water.

5.3. Potential energy surface (PES) scans of the nine **Fxx** conformers (rotamers), optimised in *gas phase [DFT - B3LYP/6-311++G(d,p)]*

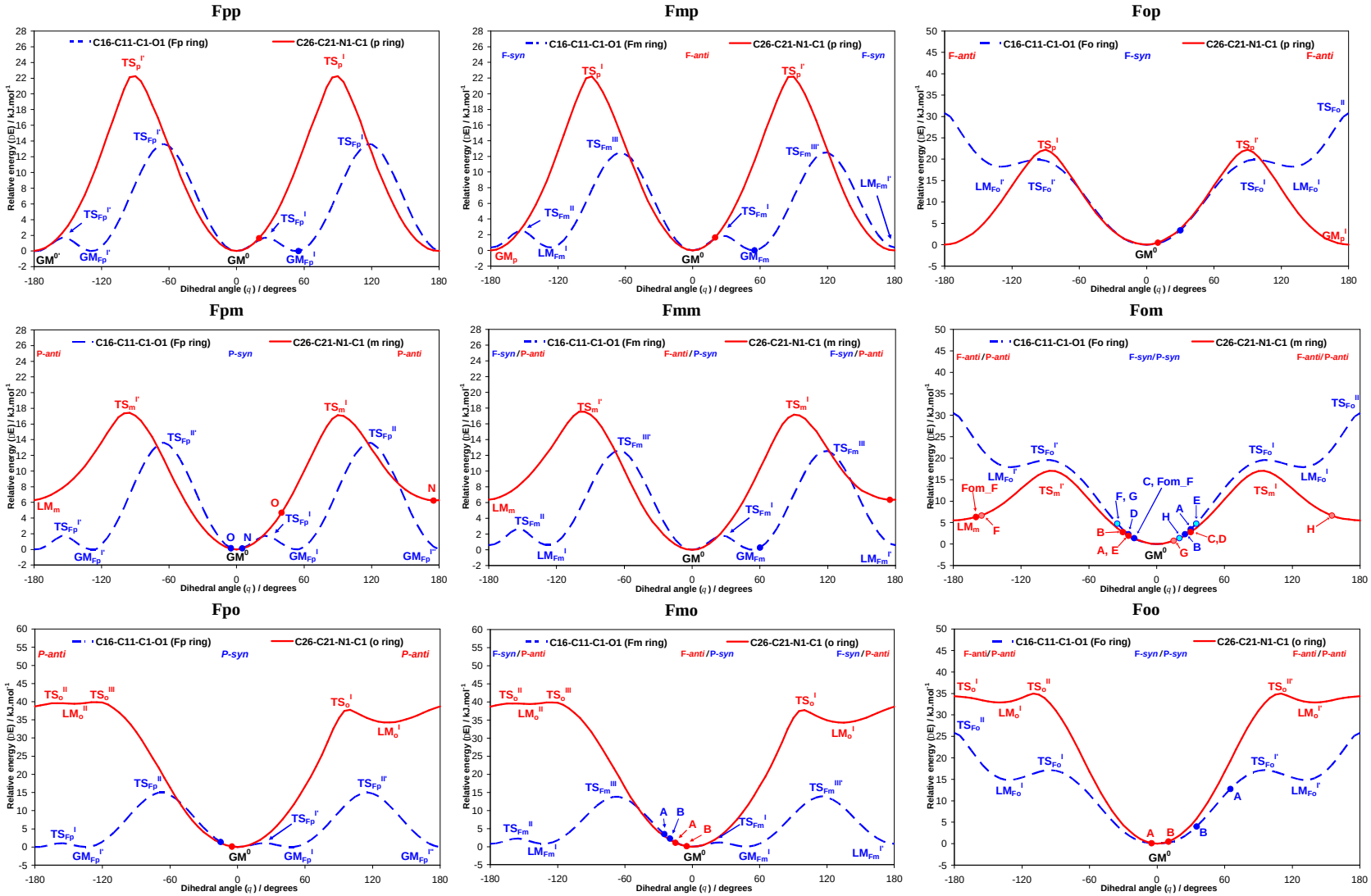
Fpp
C16-C11-C1-O1 (Fp ring)
C26-C21-N1-C1 (p ring)
Fmp
C16-C11-C1-O1 (Fm ring)
C26-C21-N1-C1 (p ring)
Fop
C16-C11-C1-O1 (Fo ring)
C26-C21-N1-C1 (p ring)
Fpm
C16-C11-C1-O1 (Fp ring)
C26-C21-N1-C1 (m ring)
Fmm
C16-C11-C1-O1 (Fm ring)
C26-C21-N1-C1 (m ring)
Fom
C16-C11-C1-O1 (Fo ring)
C26-C21-N1-C1 (m ring)
Fpo
C16-C11-C1-O1 (Fp ring)
C26-C21-N1-C1 (o ring)
Fmo
C16-C11-C1-O1 (Fm ring)
C26-C21-N1-C1 (o ring)
Foo
C16-C11-C1-O1 (Fo ring)
C26-C21-N1-C1 (o ring)
Relative energy (ΔE) / kJ.mol-1
Dihedral angle (q) / degrees

Detailed description:

The *para*-fluorophenyl (**Fp**) ring gives a PES profile with two global maxima located *ca*. -65° and 120° (TS_{Fp}^{II}[**Fpp/m**] = 13.61 ± 0.03 kJ.mol^{-1}, TS_{Fp}^{II}[**Fpo**] = 15.01 kJ.mol^{-1}), two local maxima *ca*. 25° and -155° (TS_{Fp}^{I}[**Fpp/m**] = 1.73 ± 0.03 kJ.mol$^{-1,}$ TS_{Fp}^{I}[**Fpo**] = 0.94 kJ.mol^{-1}). The four global minima are near 0°, 55°, ±180° and -130°.
Rotation of the *meta*-fluorophenyl (**Fm**) ring gives a PES profile with two global minima *ca*. 55° and 0°, two global maxima at *ca*. -65° and 120° (TS_{Fm}^{III} = 13.00 ± 0.66 kJ.mol^{-1}), two local minima *ca*. -130° and ±180° with increases of (LM_{Fm}[**Fmp**] = 0.37 kJ.mol^{-1} to LM_{Fm}[**Fmo**] = 0.83 kJ.mol^{-1}**)**. The two local maxima are at -155° (TS_{Fm}^{II} = 2.46 ± 0.17 kJ.mol^{-1}). and 25° (TS_{Fm}^{I}[**Fmp/m**] = 1.83 kJ.mol^{-1}, TS_{Fm}^{I}[**Fmo**] = 1.14 kJ.mol^{-1},)
The *ortho*-fluorophenyl (**Fo**) ring has a symmetric PES profile with one global maximum at ±180° (TS_{Fo}^{II}[**Fpo**/**Fmo**] = 30.65 ± 0.23 kJ.mol^{-1}, TS_{Fo}^{II}[**Foo**] = 25.82 kJ.mol^{-1}), two local maxima at ±95° (TS_{Fo}^{I}[**Fpo**/**Fmo**] = 19.73 ± 0.17 kJ.mol^{-1}, TS_{Fo}^{I}[**Foo**] = 17.16 kJ.mol^{-1}), two local minima at ±130° (LM_{Fo}^{I}[**Fpo**/**Fmo**] = 18.07 ± 0.19 kJ.mol^{-1}, LM_{Fo}^{I}[**Foo**] = 14.83 kJ.mol^{-1}) and one global minimum at 0°.
Rotation of the *para*-pyridyl (**p**) ring gives a PES profile with two global maxima at *ca*. ±90° (TS_{p}^{I} = 22.23 ± 0.04 kJ.mol^{-1}) and two global minima at 0° and ±180°.
The *meta*-pyridyl (**m**) ring has a PES profile with two global maxima *ca*. ±95° (TS_{m}^{I}=17.21 ± 0.22 kJ.mol^{-1}), two local minima at ±180° (LM_{m}^{I} = 6.05 ± 0.45 kJ.mol^{-1}), and one global minimum at 0°.
Rotation of the *ortho*-pyridyl (**o**) rings in **Fpo** and **Fmo** give asymmetrical PES profiles, while in the **Foo** isomer the PES profile of the **Fo** ring is symmetric. In **Fpo** and **Fmo** one global maximum is located at *ca*. -125° (TS_{o}^{III}= 39.86 kJ.mol^{-1}), two local maxima at *ca*. 100° (TS_{o}^{I}= 37.73 kJ.mol^{-1}) and *ca*. -160° (TS_{o}^{II} = 39.58 kJ.mol^{-1}), two local minimum at *ca*. 135° (LM_{o}^{I} = 34.26 kJ.mol^{-1}) and *ca*. -145° (LM_{o}^{II} = 39.44 kJ.mol^{-1}) and global minimum at 0°. However, in symmetric **Foo** there is two global maxima at ±110 º (TS_{o}^{II}[**Foo**] = 34.95 kJ.mol^{-1}), one local maximum at ±180 º (TS_{o}^{I}[**Foo**] = 34.39 kJ.mol^{-1}), two local minima at ±140 º (LM_{o} = 32.89 kJ.mol^{-1}) and one global minimum at 0°.

Additional commentary and comparisons between different basis sets

The **Fmp** and **Fmm** isomers optimised with the 6-311++G basis set have the **Fm** rings as **F-*syn***, their PES scans overwhelmingly correspond with those obtained with the polarisation function (ESI†, diagrams 5.5, 5.8). Conformational analyses with the 6-311++G basis set reveal that the **Fm** ring difference between the **F-*syn*** and **F-*anti*** conformations is even smaller (~0.1 kJ.mol^{-1}), suggesting, in this specific case, the dependence of the optimised model and conformation on a particular basis set and function choice, together with the existence of **F-*syn*/F-*anti*** equivalence. However, optimisation and conformational analyses with the 6-311G** basis set shows a preference for **F-*anti*** in the **Fm** ring for all **Fmx** isomers.

5.5. Potential energy surface (PES) scans of the nine **Fxx** conformers (rotamers), optimised in *gas phase [DFT - B3LYP/6-311++G]*

Fpp

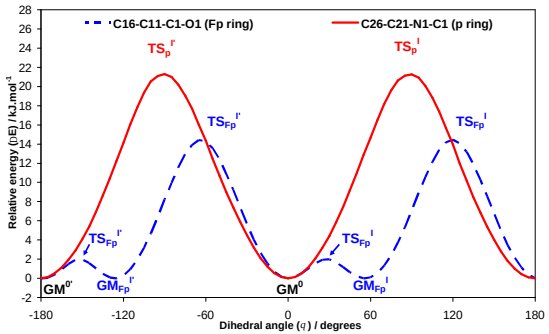

Fmp

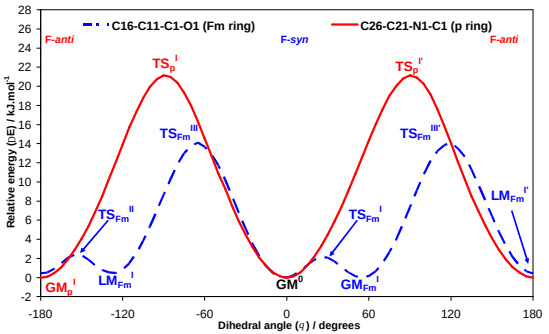

Fop

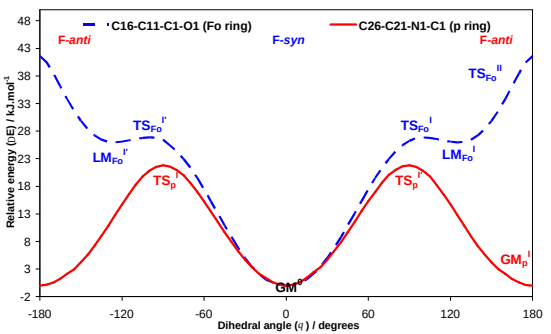

Fpm

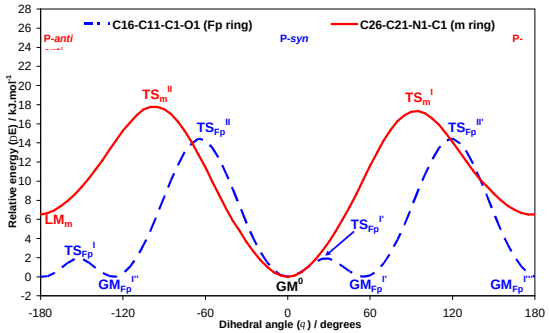

Fmm

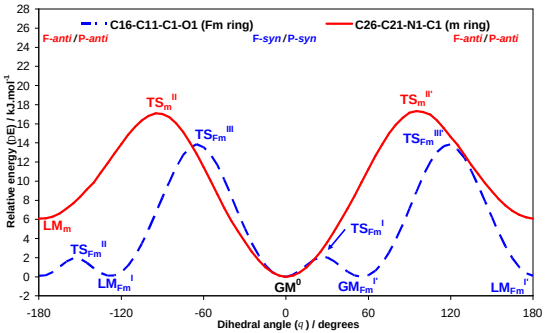

Fom

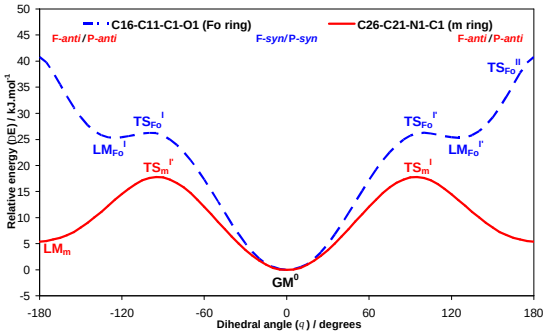

Fpo

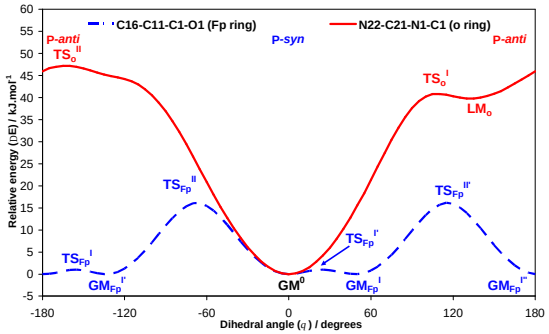

Fmo

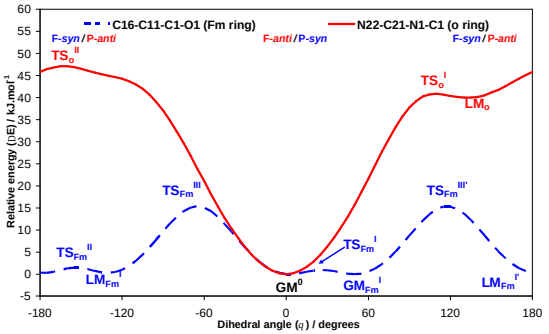

Foo

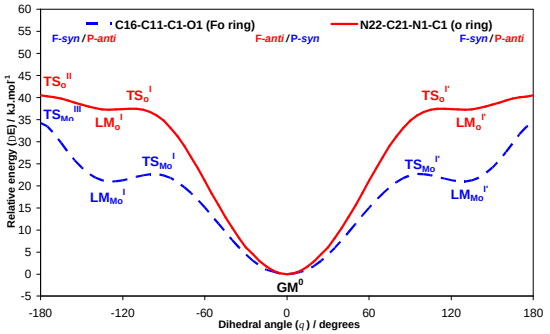

5.6. Potential energy surface (PES) scans of the nine **Fxx** conformers (rotamers), optimised in *gas phase [DFT - B3LYP/6-311G(d,p)]*

Fpp

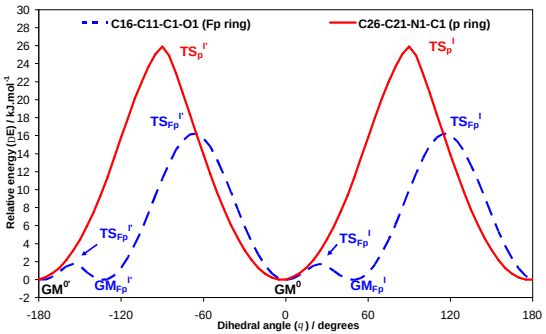

Fmp

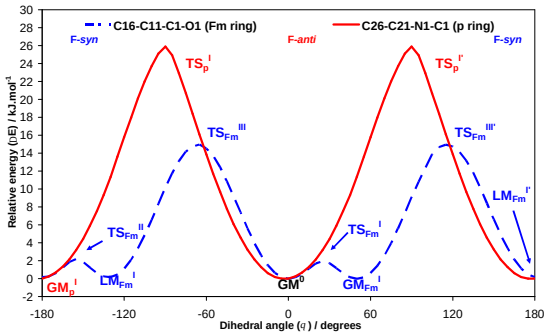

Fop

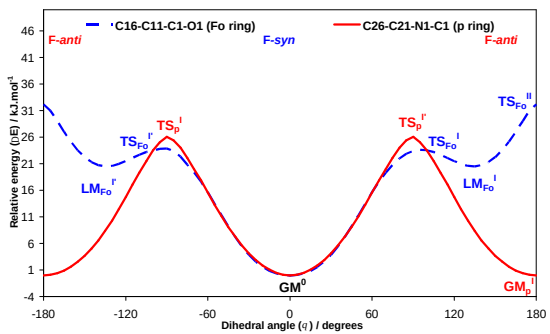

Fpm

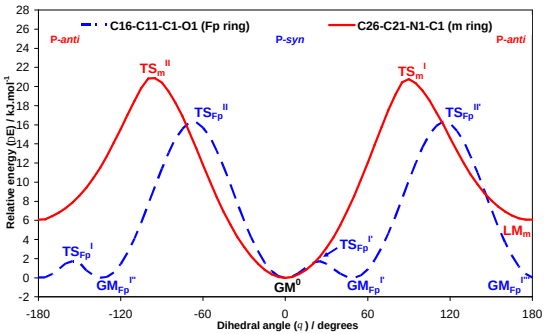

Fmm

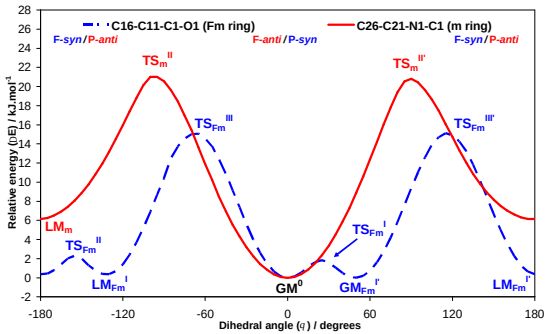

Fom

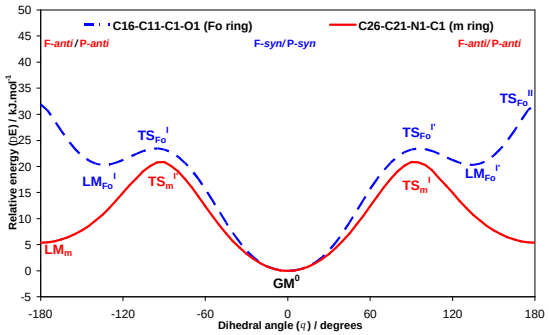

Fpo

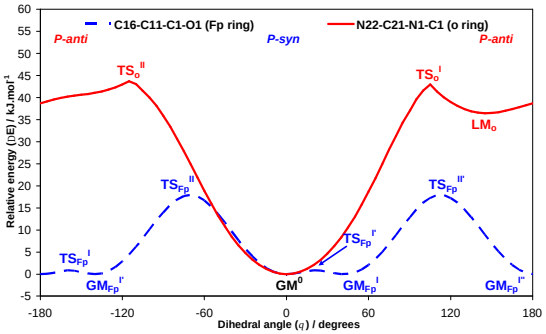

Fmo

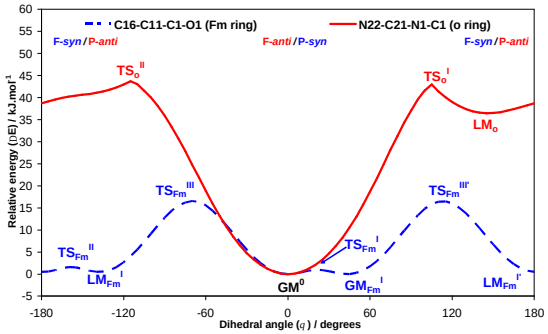

Foo

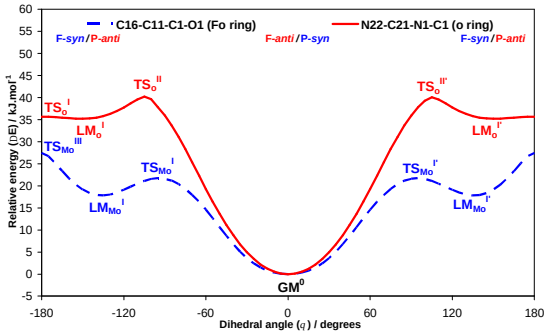

5.7. Difference in PES scans of pyridyl ring between different basis sets (*gas phase*)

Fpp

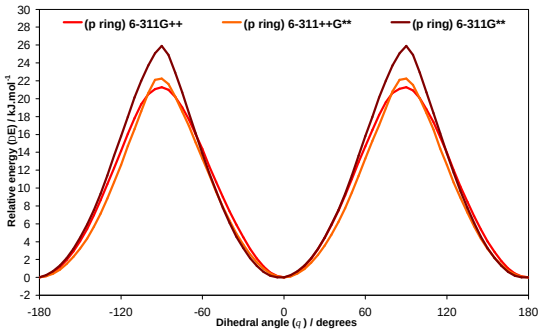

Fmp

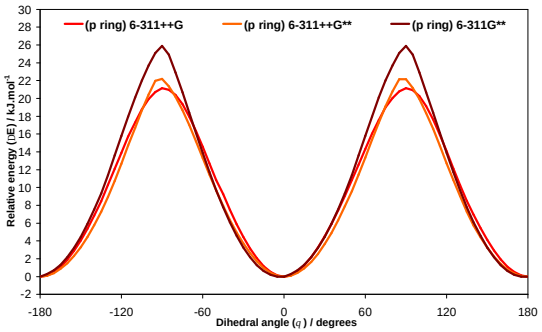

Fop

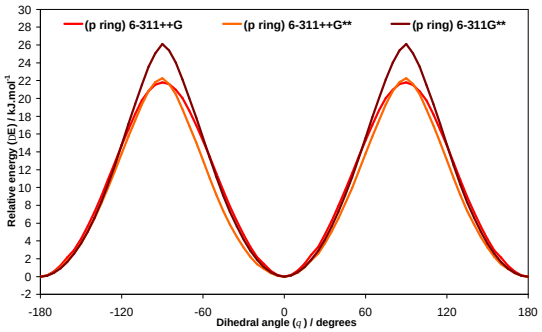

Fpm

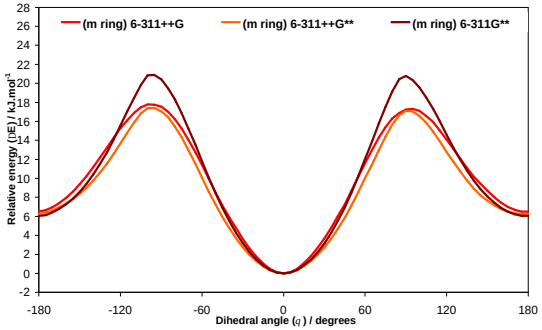

Fmm

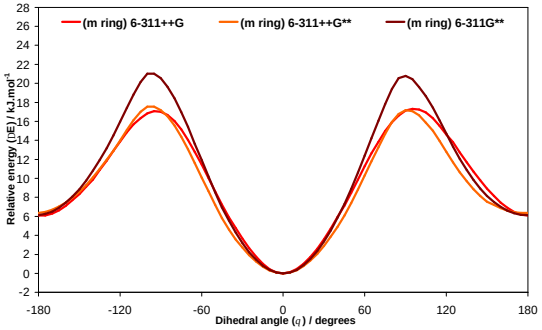

Fom

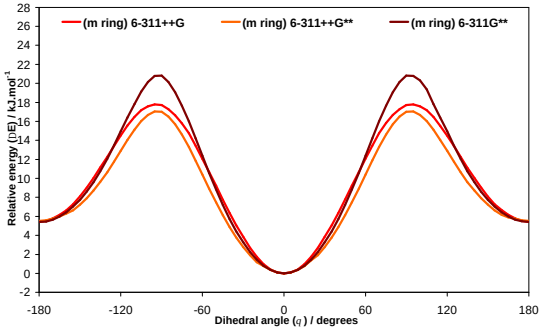

Fpo

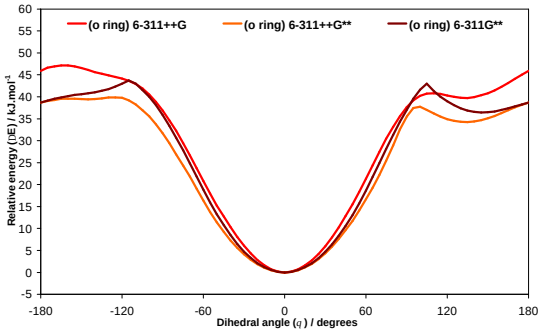

Fmo

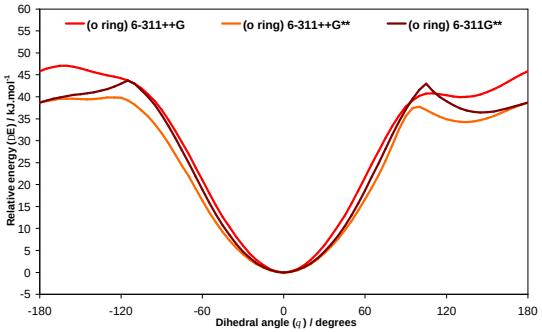

Foo

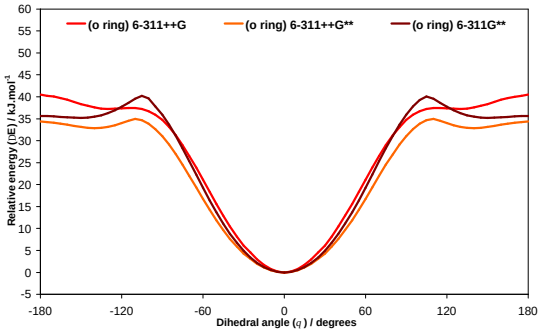

5.8. Difference in PES scans of fluorophenyl ring between different basis sets (*gas phase*)

Fpp

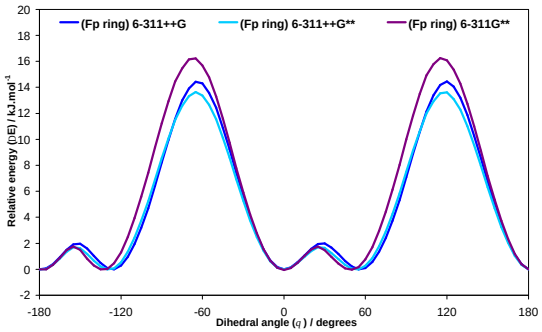

Fmp

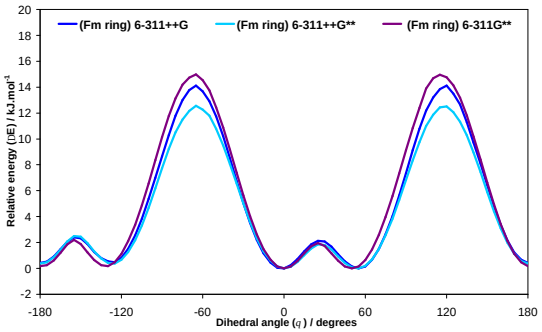

Fop

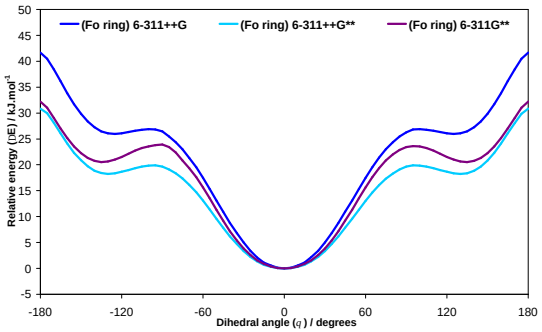

Fpm

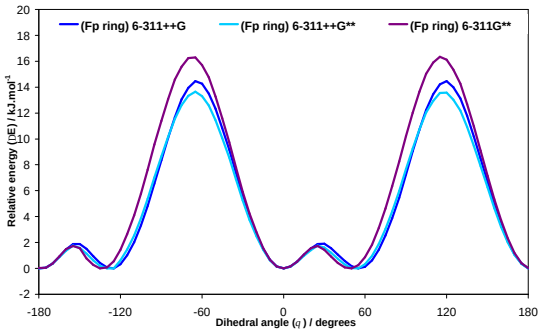

Fmm

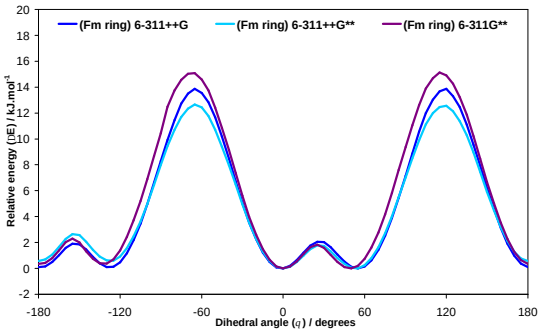

Fom

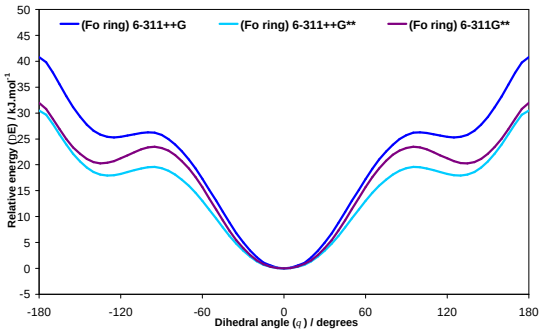

Fpo

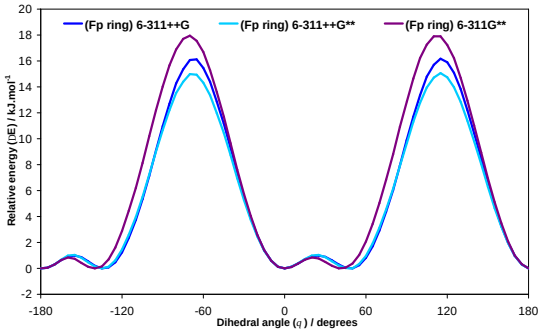

Fmo

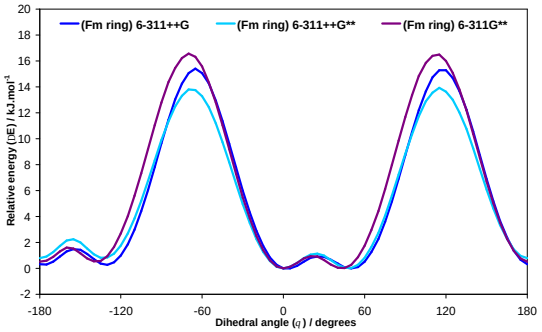

Foo

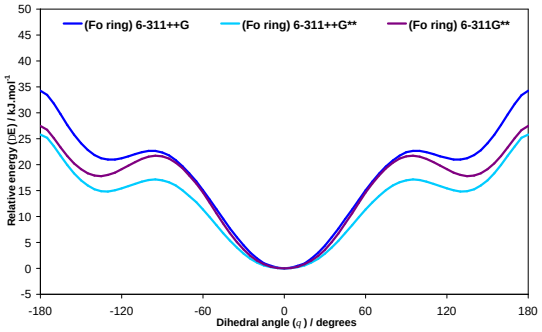

5.9. PES scans of the **Fx** rings of the nine **Fxx** conformers (rotamers), optimised in *gas phase* (full line), CH_2Cl_2 (DCM, dashed line) and in H_2O (dotted line).

Fpp

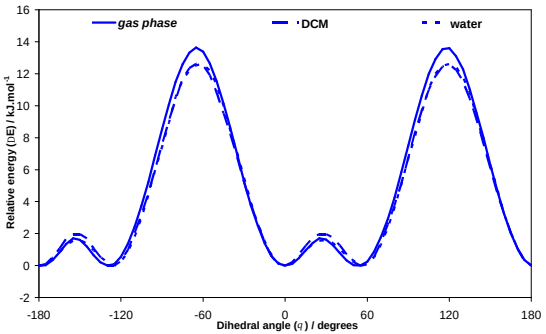

Fmp

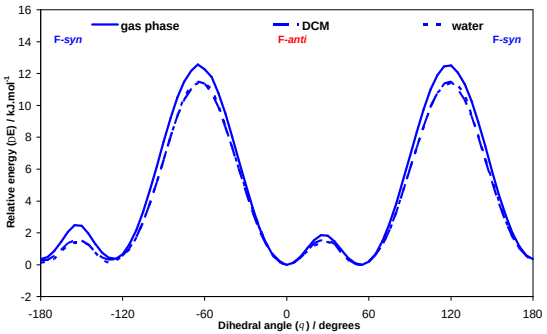

Fop

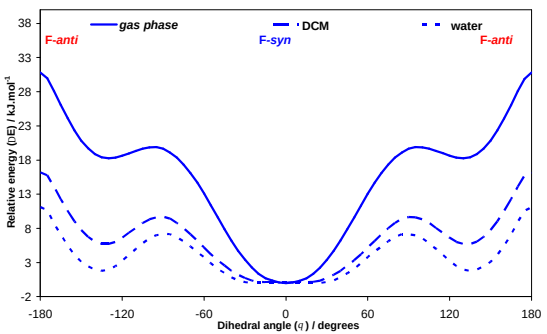

Fpm

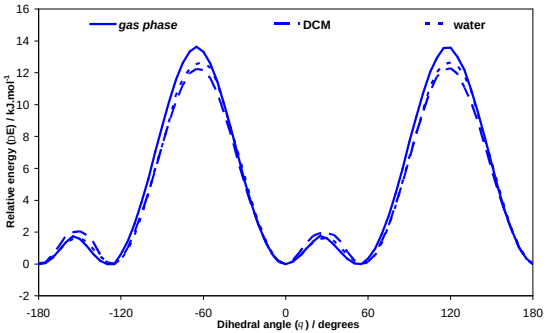

Fmm

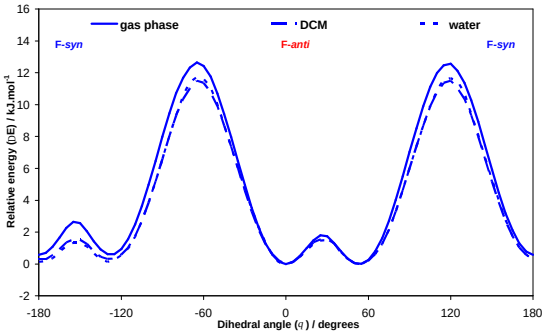

Fom

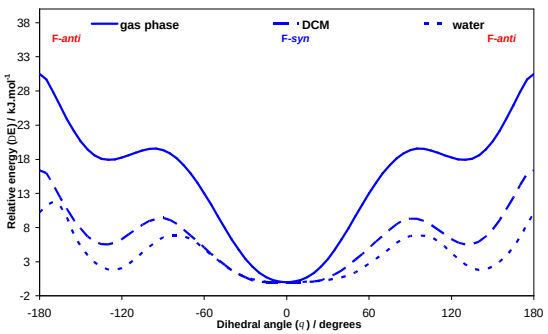

Fpo

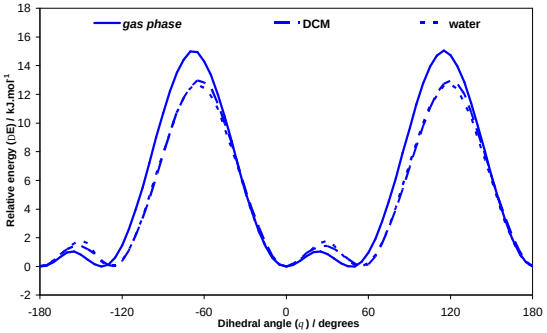

Fmo

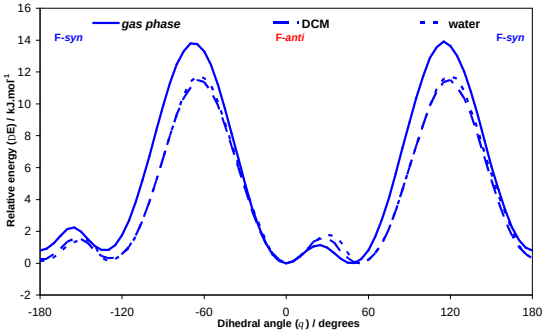

Foo

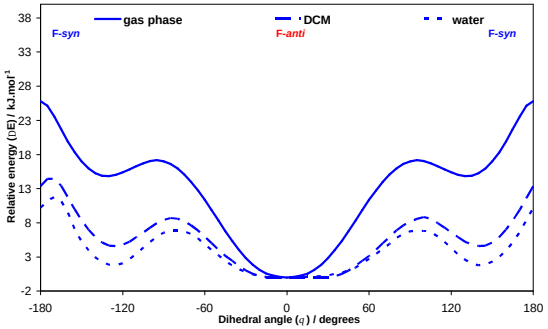

Detailed description:

The main characteristic of the PES of **Fx** rings in different solvents when compared with the corresponding PES *gas phase* is the uneven difference in the decrease/increase of the rotational barriers and local minima throughout the **Fxx** isomer grid. This is already seen in the **Mxx** isomer grid, however, the **Fo** ring, forming an intramolecular hydrogen bond with the amide proton has a specific pattern of behaviour that resembles the **oF** ring in the **NxxF** isomer grid. Therefore, concerning the PES of **Fx** ring in solvents, the isomers can be divided in three groups: **Fpp**/**m**, **Fmp**/**m**, **Fox**, while **Fpo** and **Fmo** have slightly different patternd compared to the **Fpx** and **Fmx** triads and will be explained separately. However, it is clear that the influence of solvents is minor in the **Fp** and **Fm** rings (especially in **Fpp**/**m** and **Fmp**/**m**) while in **Fo** a strong decrease is observed. In **Fpp**/**m** the influence of solvents on PES of **Fp** ring is minor, the main rotational barrier TS_{Fp}^{II} decreases by ~9 % in CH_2Cl_2 (~7 % in H_2O). On the other hand, TS_{Fp}^{I} increases by ~14 % in CH_2Cl_2 (decrease of ~7 % in H_2O). This phenomenon is already seen in the **Mxx** isomers and can be explained partially by the fact that TS_{Fp}^{I} represents molecules in planar conformations, and higher dielectric field may destabilise molecules in such conformations. The reason for the decrease in the case of H_2O is perhaps an artefact. In **Fpo** the decrease of TS_{Fp}^{II} is more significant, ~14% in CH_2Cl_2 (~15.5% in H_2O) as well as increases of TS_{Fp}^{I} (~36% in CH_2Cl_2, ~71% in H_2O). However, there is a striking similarity between the PES of the **Fp** and **Mp** rings. The behaviour of the PES for the **Fm** ring in **Fmp**/**m** isomers is slightly different than in **Fp**. There is a similar small drop in the main rotational barrier TS_{Fm}^{III} (~8 % in both solvents), however, there is clearly a decrease in TS_{Fm}^{I} (~14% in CH_2Cl_2, ~20% in H_2O). Even though the increase is expected as in the **Fp** ring or at least a partial situation as in the **Mm** ring, a decrease might be an artefact and/or result of statistical error. Nevertheless, there is a significant decrease in LM_m (~15 % in CH_2Cl_2, ~62 % in H_2O) and TS_{Fm}^{II} (~37 % in CH_2Cl_2, ~46 % in H_2O) that effectively equalises the **Fm** and **Fp** rings in a high dielectric solvent. In the case of the **Fo** ring, the behaviour in solvent seems quite even for all three **Fox** isomers. Contrary to the **Fp** and **Fm** rings, solvation strongly influences the rotational barriers producing a pronounced decrease. Further, there is no increase of the rotational barriers. The highest rotational barrier TS_{Fo}^{II} decreasing by ~46 % in CH_2Cl_2 (~62 % in H_2O) while rotational barriers TS_{Fo}^{I} decrease ~51 % in CH_2Cl_2 (~62 % in H_2O). The local minima LM_{Fo} decrease by ~69 % in CH_2Cl_2 (~89 % in H_2O). This pronounced decrease of the PES reflects the breakage of the internal hydrogen bonding (N-H...F). A similar behaviour is detected in the **oF** ring in the **NxxF** isomer grid where intramolecular N-H...F bonding was also observed.

Comparisons using different basis sets:

Conformational analyses without the polarisation (**/d,p) or diffuse (++) functions (ESI†, diagrams 5.5, 5.7-5.8) generally give analogous PES diagrams with an increase of the main rotational barriers and energies at unstable conformational states. The PES scans without the polarisation function (as 6-311++G) give, in general, higher rotational barriers except for the **p** ring where a decrease is noted. These changes are essentially insignificant in the **Fp** (~6%), **Fm** (~11%), **p** (~-4%) and **m** rings (~2%), while for the **Fo** (~37%) and **o** rings (~16%) the rotational barrier increase is more pronounced with a slight change in the PES curve shape. This reflects the influence of polarisation on the interactions of electronegative atoms (F) and protons in molecules, as well as on intramolecular interactions (N-H...F_{ortho}). In contrast, conformational analyses without the diffuse function (as 6-311G**) substantially increases the main rotational barriers but the pattern is opposite to the 6-311++G basis set with increases in **Fp** (~20%), **Fm** (~20%), **p** (~16%) and **m** rings (~20%) but lower in the **Fo** (~16%) and **o** rings (~8%) suggesting the importance of the diffuse function in energy estimation in the transition states of these molecular systems. As there is no conformational change (***syn***/***anti***) in any ring with the 6-311G** basis set it may be concluded that polarisation functions represents an important auxiliary addition for model stability if flexibility and conformational change are important.

Detailed description:

Conformational analyses of the pyridinyl rings with SMD solvation model shows significant decreases of the rotational barriers and local minima in both solvents (CH_2Cl_2 and H_2O).

For the *para*-pyridyl rings (**p**) the decrease in CH_2Cl_2 is 8.29% and in H_2O is 18%, and a slight shift in TS_p by 10º is observed. In the case of the *meta*-pyridinyl rings (**m**) the rotational barriers decreases by 24.65% in CH_2Cl_2 (44.8% in H_2O) while LM_m decreases by 60.21% in CH_2Cl_2 (80.25% in H_2O). In the *ortho*-pyridyl rings (**o**) there is an almost even decrease for both barriers and local minima by 39.41% in CH_2Cl_2 (63.20% in H_2O).

5.10. PES scans of the **xAP** rings of the nine **Fxx** conformers (rotamers), optimised in *gas phase* (full line), CH_2Cl_2 (DCM, dashed line) and in H_2O (dotted line).